

Phylogeny of the riodinid butterfly subtribe Theopeina (Lepidoptera: Riodinidae: Nymphidiini)

JASON P. W. HALL

Department of Systematic Biology–Entomology, National Museum of Natural History, Smithsonian Institution, Washington, DC, U.S.A.

Abstract. The almost exclusively Neotropical butterfly family Riodinidae is poorly represented in both ecological and systematic studies of Lepidoptera. A comparative morphological study of all seventy-five species in subtribe Theopeina (tribe Nymphidiini) yielded 104 characters, predominantly from wing pattern, male and female genitalia, and abdominal structures. All morphological characters and adults representing the range of wing pattern variation are illustrated. Phylogenetic analysis of the data produced a large number of most parsimonious cladograms, but the strict consensus of these, both when using equal weights and after successive weighting, is well resolved and the majority of terminal clades have high character and branch support. Theopeina is found to consist of five monophyletic genera, *Protonymphidia*, *Archaeonympha*, *Calicosama*, *Behemothia* and *Theope* (= *Parnes* and *Dinoplotis*), with the largest genus *Theope* containing thirteen monophyletic species groups, which are delineated to facilitate a discussion of broad evolutionary patterns in this morphologically diverse subtribe.

Introduction

Riodinidae are unique among butterflies in being almost exclusively confined to a single biogeographical region, the Neotropics, where approximately 1300 species or 95% of the familial diversity occurs, and where it constitutes about 20% of the total butterfly fauna (Robbins, 1982, 1993; Heppner, 1991; Robbins *et al.*, 1996). The family is conspicuous not only for its species diversity, but also for its great morphological and ecological diversity. Its biology is perhaps the most poorly known of any butterfly group, yet the study of riodinids promises to provide key insights into several aspects of evolutionary biology. These include mimicry-driven phenotypic plasticity, mimicry being perhaps more rampant in this family than in any other (Bates, 1859; Seitz, 1916–20; d'Abrera, 1994; Miller, 1996), the maintenance of reproductive isolation through highly species-specific male perching behaviours (Callaghan, 1983; Brévignon & Gallard, 1995; Hall, 1999a), and myrmecophily and related attributes of larval life history strategies (DeVries, 1988, 1990, 1991a,b,c, 1997). However, there are currently no detailed tribal or subtribal phylogenies for the

family upon which to trace major evolutionary adaptations or test competing hypotheses.

The first higher classification of Riodinidae was attempted by Bates (1868), who recognized three subfamilies and several further divisions based solely on characters of wing venation, antennae and palpi. However, his classification was not followed by subsequent authors and it was not until the following century that Stichel (1910, 1911, 1928, 1930–31), using a broader range of external and internal characters, produced the first widely accepted classification, recognizing two subfamilies and many tribal and subtribal divisions. The first attempt at a 'modern', natural classification, based on monophyletic groups, was that of Harvey (1987), who recognized five subfamilies and eleven tribes (now reduced to nine, see Hall, 1998b, 1999a) for one of them, Riodininae. Based on the most extensive examination of internal and external adult and early stage morphological characters to date, this classification provided the platform on which to base more detailed systematic studies (Hall & Willmott, 1995a,b, 1996a,b, 1998a,b; DeVries & Hall, 1996; Brévignon & Gallard, 1997a,b, 1998a,b,c; Callaghan, 1997; Hall & Harvey, 1998; Hall, 1998a,b, 1999a, 2000; Penz & DeVries, 1999).

The purpose of this paper is to begin the process of delineating monophyletic groups in Riodinidae below the tribal level and of elucidating phylogenetic relationships among them using cladistic methods. It is only then that a natural generic classification can be proposed and the main

Correspondence: Jason Hall, Department of Systematic Biology–Entomology, National Museum of Natural History, Smithsonian Institution, Washington, D.C. 20560-0127, U.S.A. E-mail: jpwHall@hotmail.com

impediment to our understanding of character evolution in the group removed. Specifically, the tribe of interest here is Nymphidiini Bates (*sensu* Hall, 1999a), by far the largest in the family (over 300 species), and, exacerbated by its large number of very rare species, probably the least understood systematically of all the tribes (Harvey, 1987). As one of only two myrmecophilous tribes in Riodinidae (the other is the distantly related Eurybiini Reuter (Harvey, 1987; Campbell, 1998; Campbell *et al.*, 2000)), studies of Nymphidiini have provided a deeper understanding of riodinid-ant symbioses and communication systems between caterpillars and ants (DeVries, 1990, 1991a,c, 1997; DeVries *et al.*, 1994).

Harvey (1987) diagnosed Nymphidiini on the basis of its members possessing a ventrally rather than dorsally positioned spiracle on male abdominal segment 3, and he placed it as the sister tribe to Lemoniadini Kirby (= Lemoniini Auctt., see Hall & Heppner, 1999) on the basis of several shared apomorphies of larval morphology relating to myrmecophily. However, given the weak character support for Lemoniadini (Hall, 1999b; Penz & DeVries, 1999) and its probable paraphyly (as currently conceived) with respect to Nymphidiini (Hall, 1999b), the two tribes were synonymized by Hall (1999a) and subsequently Penz & DeVries (1999). Given its size and morphological diversity, Hall (1999a) recognized three subtribes for Nymphidiini, Nymphidiina Bates, Theopeina Clench (both formerly part of Harvey's, 1987, Nymphidiini), and Lemoniadina Kirby. This paper presents a comprehensive morphological phylogenetic analysis for subtribe Theopeina, which is characterized by the universal absence of dorsal sclerotized tissue (often termed a transtilla) joining the distal portion of the valvae of the male genitalia (this is present in members of Nymphidiina), a dorsally incomplete vinculum at the anterior edge of the tegumen (not in *P. senta* Hewitson, 1853, and found elsewhere only in two genera of Nymphidiina) and the lack of a saccus (absent in all genera but *Calicosama* Hall & Harvey, 2001) (Hall, 1999a; unpublished data).

Methods

Taxa studied

Recently, there has been increasing interest in the effect of taxon sampling on the resulting phylogenetic hypothesis. The general consensus is that judicious addition of taxa is likely to give better resolution on the cladogram (Hendy & Penny, 1989; Lecointre *et al.*, 1993; Hillis, 1996, 1998; Graybeal, 1998), and will typically lead to the useful elimination of previously unwittingly used spurious characters and character states. Of course, even the omission of as yet undiscovered species and extinct species (see DeVries & Poinar, 1997; for an illustration and discussion of a fossilized putative *Theope* larva) can adversely affect the accuracy of the phylogenetic hypothesis. Nevertheless, the extant taxon saturation approach is the best available and is the one adopted here as the surest method of elucidating

the monophyly of genera and their phylogenetic relationships. Thus, all seventy-five species (see Figs 1 and 2 for representatives) identified as belonging to subtribe Theopeina were incorporated into this analysis. These include the one species of *Protonymphidia* Hall, 2000, three *Archaeonympha* Hall & Harvey, 1998, two *Calicosama* Hall & Harvey, 2001, one *Behemothia* Hall, 2000, and sixty-eight *Theope* Doubleday, 1847 (Hall & Harvey, 1998, 2001; Hall, 1999a, 2000). Notably, *Theope* is the largest genus in the tribe and also the third largest in the family after *Euselasia* Hübner, [1819], and *Mesosemia* Hübner, [1819] (Bridges, 1994; Hall, 1999a). Capture localities and institutional locations of all *Theope* specimens examined (4241) and dissected (240) were listed in Hall (1999a), and those for the remaining genera are listed in Table 1. A list of all *Archaeonympha* specimens examined is given by Hall & Harvey (1998). *Thisbe irenea* (Stoll, [1780]) was designated as the outgroup because the dorsally positioned spiracle on abdominal segment 3 in males places it outside the ingroup, in the nymphidiine subtribe Lemoniadina, but its genital morphology is still sufficiently similar to that of the ingroup to aid character homology.

Morphology

The phylogenetic analyses in this paper are based largely on characters from the internal and external morphology of adults of both sexes, gleaned from specimens collected by myself in Ecuador and from those in fourteen institutions and private collections in Europe, North America and South America (listed in Hall, 1999a). Characters of early stage larvae and pupae would undoubtedly provide additional phylogenetic information, as they have done in several other cladistic studies of Lepidoptera (Kitching, 1985; Brown & Freitas, 1994; Miller, 1996; Parsons, 1996; Penz, 1999), but early stage material is available for only nine of the species studied, eight *Theope* species and *Protonymphidia senta* (Guppy, 1904; Harvey, 1987; DeVries *et al.*, 1994; DeVries, 1997; Hall, 1999a), an insufficient 12% of the ingroup.

Dissections were performed using standard techniques, after having placed abdomens in hot 10% potassium hydroxide solution for approximately 10 min, and the resulting material was stored in glycerol after examination. All characters were scored using light microscopy, but a few were also examined with a Hitachi S4000 digital scanning electron microscope by rinsing in water and air drying material that was stored in glycerol and mounting it on stubs using carbon tape. The terminology for male and female genital and abdominal structures follows Klots (1956) and Eliot (1973), and nomenclature for wing venation follows Comstock & Needham (1918).

Cladistic analyses

A total of 104 characters, sixty-seven binary and thirty-seven multistate (Appendix 1) were used in the analysis.

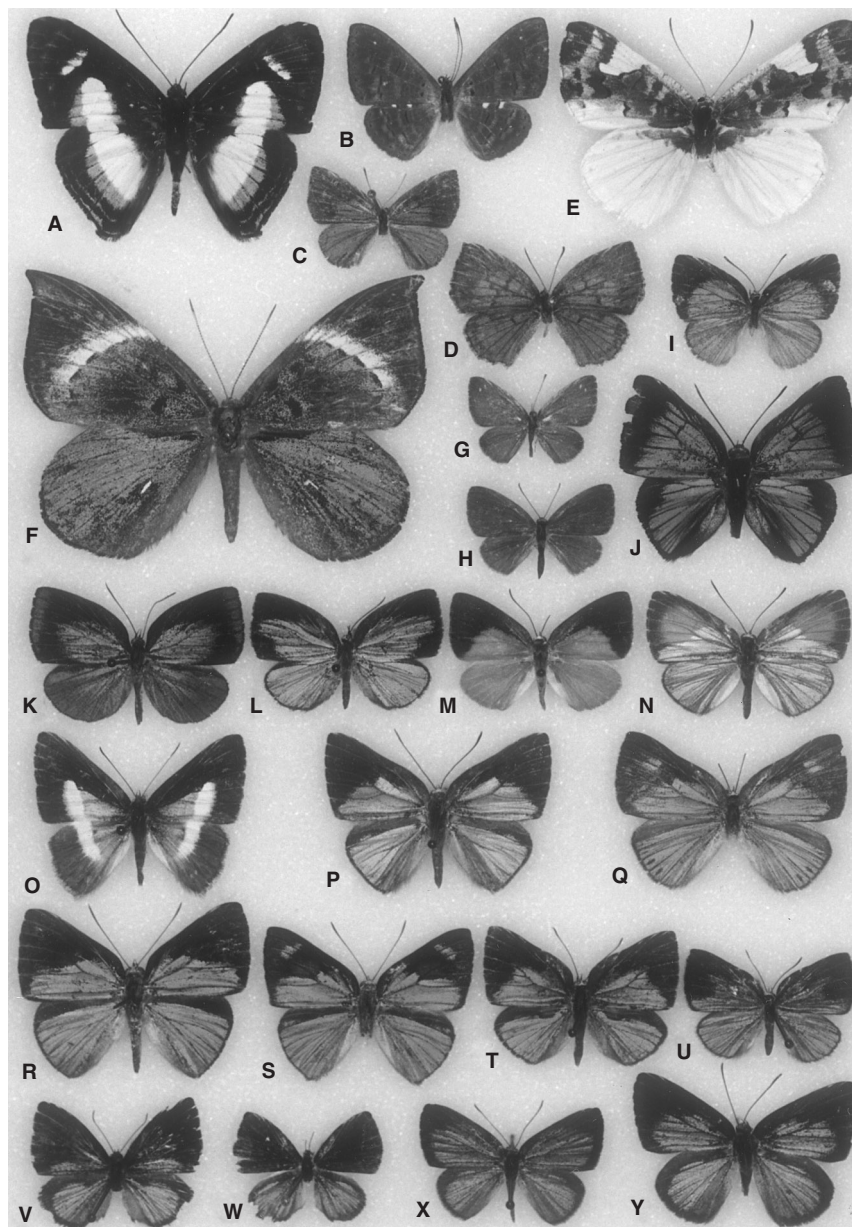


Fig. 1. Sample of taxa representing members from all genera and all species groups within the largest genus *Theope* (clades 1–13 in Fig. 3 and marked here). Wing shape, dorsal wing pattern and dorsal abdominal characters 2–11 and 31–32 from Appendix 1 are illustrated here. All specimens are males unless otherwise stated. A, *Thisbe irenea* (outgroup taxon); B, *Protonymphidia senta*; C, *Archaeonympha smalli*; D, *Archaeonympha urichi*; E, *Calicosama lilina*; F, *Behemothia godmanii*; G, *Theope brevignoni* (1); H, *Theope tetrastigma* (2); I, *Theope hypoleuca* (3); J, *Theope matuta heureka* (4); K, *Theope pepo* (5); L, *Theope pepo* (female) (5); M, *Theope acosma* (6); N, *Theope aureonitens* (6); O, *Theope sisemina sisemina* (7); P, *Theope virgilius* (8); Q, *Theope virgilius* (female) (9); R, *Theope basilea* (10); S, *Theope publius publius* (10); T, *Theope sobrina* (11); U, *Theope sobrina* (female) (11); V, *Theope decorata* (12); W, *Theope decorata* (female) (12); X, *Theope lycaenina* (13); Y, *Theope wallacei* (13).

Phylogenetically uninformative autapomorphies, given by Hall (1999a) for *Theope* species, were omitted. Initial analysis of the data (Appendix 2) was performed using a heuristic search, with TBR branch-swapping, in PAUP 4.0b4a (Swofford, 1999). All characters were weighted equally and multistates treated as unordered, therefore making no

a priori assumptions about the relative importance of characters or the evolutionary history of their component states. As a large number of equally most parsimonious cladograms (MPCs) was generated, and given computer memory constraints, the initial search had to be curtailed. Such subsamples of the total number of cladograms have

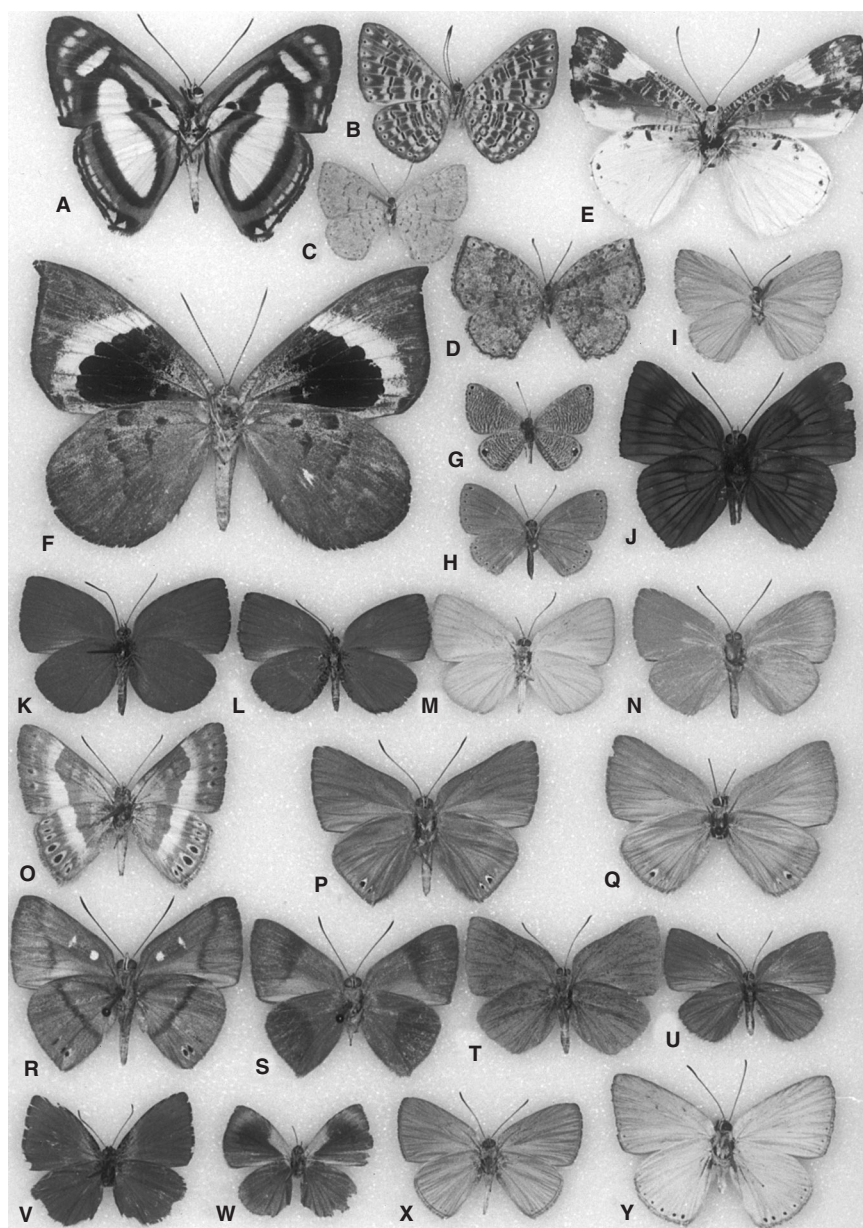


Fig. 2. Same sample of taxa shown in Fig. 1, illustrating ventral wing pattern and ventral abdominal characters 12–30 and 33 from Appendix 1.

been shown to yield very similar or typically identical topologies to consensus cladograms for the total (i.e. the phylogenetic signal is highly similar throughout the course of branch swapping) (Naylor, 1992; Liebherr & Zimmerman, 1998). However, to reduce the likelihood that any 'islands' (*sensu* Maddison, 1991) of shorter cladograms were overlooked during this truncated search, a second analysis of 2000 heuristic searches with random addition sequences was conducted (with the Multrees option deactivated). A posteriori reweighting, in the form of successive approximations character weighting (SACW) (Farris, 1969; Carpenter, 1988), was subsequently

implemented using the rescaled consistency index of each character.

Although there are certain statistical objections (e.g. see Sanderson, 1995) for using bootstrap analysis to assess the strength of branch support (Felsenstein, 1985), it remains widely utilized, and branch support was partially estimated here by means of 1000 bootstrap replicates in PAUP. Additional branch support was estimated using decay indices (Bremer, 1988, 1994) computed using PAUP in combination with AUTODECAY 4.0 (Eriksson, 1998). Character distribution was studied using MacClade 3.05 (Maddison & Maddison, 1995).

Table 1. Taxa and dissections examined exclusive of *Theope* (see Appendix 2 for list of *Theope*; Hall, 1999a, lists all dissections examined in this genus). The male of *Archaeonympha urichi* and the female of *Calicosama robbinsi* are unknown. The following collection acronyms are used: FSCA, Florida State Collection of Arthropods, Division of Plant Industry, Gainesville, FL, U.S.A.; JHKW, Collection of Jason P. W. Hall and Keith R. Willmott, Washington, DC, U.S.A.; USNM, National Museum of Natural History, Smithsonian Institution, Washington, DC, U.S.A.; ZMHU, Zoologische Museum für Naturkunde, Humboldt Universität, Berlin, Germany.

Taxon	Dissections examined
<i>Thisbe irenea</i> (Stoll, [1780]) (outgroup)	1♂: Panama, Canal Zone, Gamboa (USNM); 1♂: Ecuador, Napo, Pimpilala (JHKW); 1♂, 1♀: Panama, Canal Zone, Cocoli (USNM); 1♀: Ecuador, Manabí, Ayampe (JHKW)
<i>Protonymphidia senta</i> (Hewitson, [1853])	2♂, 1♀: Brazil, Rondônia, nr Cacaupê (FSCA); 1♀: Ecuador, Napo, nr Misahuallí (JHKW)
<i>Archaeonympha smalli</i> Hall & Harvey, 1998	2♂: Panama, Canal Zone, Cocoli (USNM); 1♀: Panama, Canal Zone, Cocoli (USNM)
<i>Archaeonympha drepana</i> (Bates, 1868)	1♂, 1♀: Brazil, Amazonas, Manicoré (ZMHU)
<i>Archaeonympha urichi</i> (Vane-Wright, 1994)	1♀: Panama, Panamá, nr El Llano (USNM)
<i>Calicosama lilina</i> (Butler, 1870)	2♂: Panama, Canal Zone, Madden Forest (USNM); 1♂: Panama, Canal Zone, Paraiso (FSCA); 1♀: Panama, Canal Zone, Paraiso (USNM); 1♀: Mexico, San Luis Potosí, El Salto Falls (FSCA)
<i>Calicosama robbinsi</i> Hall & Harvey, 2001	2♂: Panama, Canal Zone, Gamboa, Cerro Pelado (USNM)
<i>Behemothia godmanii</i> (Dewitz, 1877)	1♂: Mexico, Veracruz, Paso San Juan (USNM); 1♀: Mexico, Veracruz, Rinconada (USNM)

Table 2. Universal synapomorphies (or autapomorphies) for the genera of Theopeina. The numbers in parentheses after each taxon represent the number of species it contains, the numbers in parentheses after apomorphies refer to the character number and state in this study (see Appendix 1), and the symbols (–) and (+) refer to apomorphies unique to Theopeina only and Theopeina + Nymphidiina, respectively. Reference is given to figure numbers where appropriate.

Taxon	Synapomorphies/autapomorphies
<i>Protonymphidia</i> (1)	Dorsal surface a mottled orange pattern (5:1) (–) (Fig. 1B) Spiracle on abdominal segment 3 of males positioned medially (34:1) (–) (Fig. 6B) Uncus of male genitalia very long (+) Posterior margin of uncus of male genitalia sharply notched in dorsal view (–) Falces of male genitalia very long and narrow (59:1) (+) (Fig. 9H) Valvae of male genitalia narrow, elongate and downwardly pointed (67:0) (–) (Fig. 10A) Signa of female genitalia consist of sclerotized bands on surface of corpus bursae instead of invaginations (101:0) (–) (Fig. 12E)
<i>Archaeonympha</i> (3)	Ductus bursae of female genitalia possesses an elongate, hollow, posteriorly medially divided, sclerotized structure opposite opening of ductus seminalis (95:1) (+) (Fig. 13C)
<i>Calicosama</i> (2)	A white triangle at middle of dorsal forewing costa present (6:1) (–) (Fig. 1E) Posterior portion of last male sternite heavily sclerotized and produced into 2 long, asymmetrical points (46:1) (+) (Fig. 7B) Valvae of male genitalia broad with single broad, 'bird's-head'-shaped upper projection (67:2) (+) (Fig. 10C) Soft tissue at anterior tip of aedeagus of male genitalia directed ventrally instead of anteriorly (77:1) (–) (Fig. 11C) Aedeagus of male genitalia contains long band of oval-shaped cornuti (79:1) (+) (Fig. 11C)
<i>Behemothia</i> (1)	Forewing apices produced into long points (–) (Fig. 1F) Narrow, white, curving postdiscal band on forewing present (–) (Fig. 1F) Posterior portion of last male sternite heavily sclerotized and produced into 2 short, symmetrical points (–) Valvae of male genitalia broad with concave distal margin (67:1) (+) (Fig. 10D) Aedeagus of male genitalia contains single large crescent-shaped cornutus (79:3) (+) (Fig. 11A)
<i>Theope</i> (68)	Two spots at base of cell Cu2 on ventral forewing absent (20:1) (–) (see Fig. 2) A continuous, well sclerotized dorsal invagination joins eighth male sternite to genital armature (44:2) (+) (Fig. 8A)

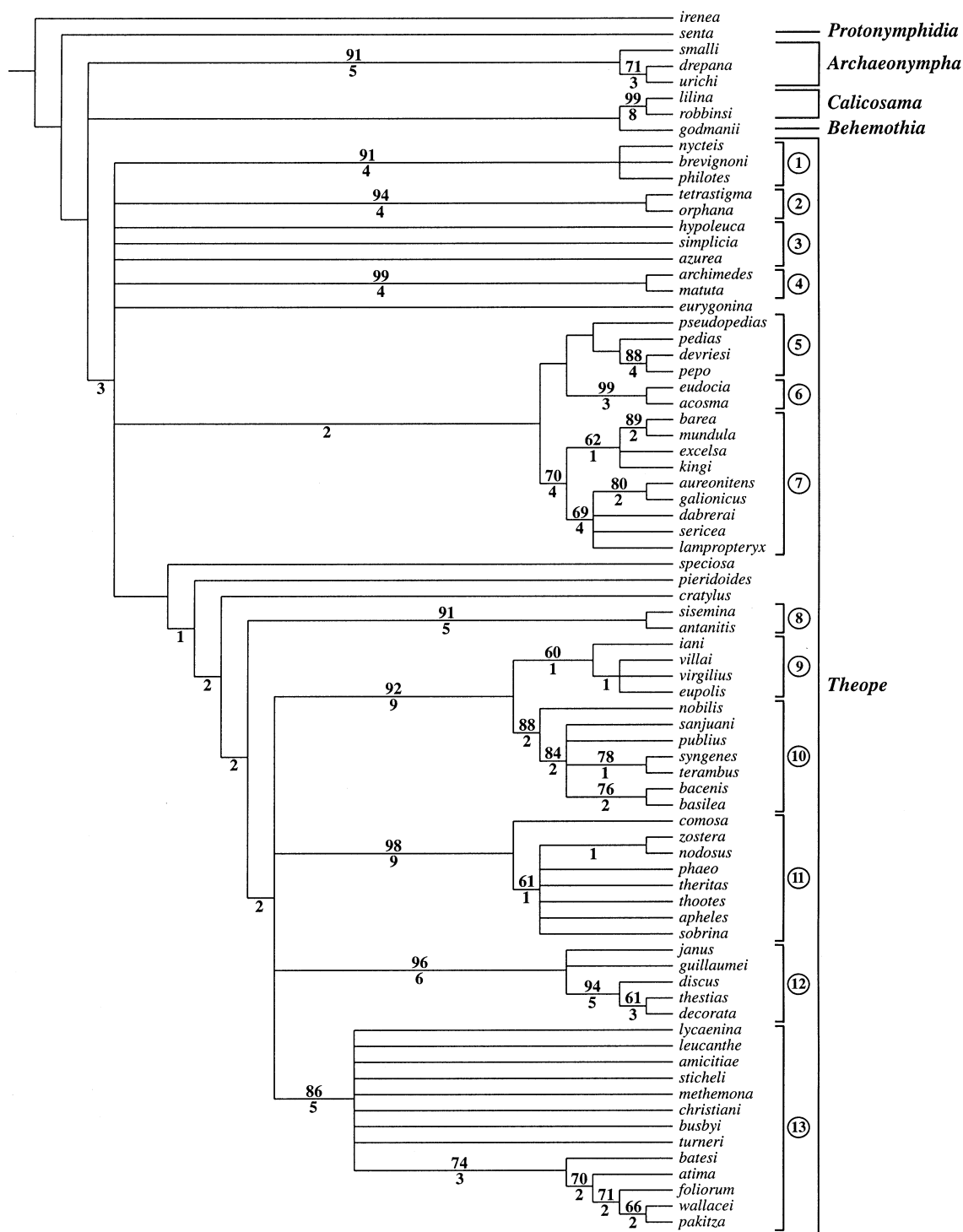


Fig. 3. Strict consensus of 116 500 equally parsimonious cladograms with equal weights for subtribe Theopeina, based on the characters in Appendix 1. Universal synapomorphies for all genera and *Theope* species groups (marked with the encircled numbers 1–13) are listed in Tables 2 and 3, respectively. Branch support is estimated using bootstrap values higher than 50 above relevant branches, and decay index values below branches. *Theope* species groups recognized by Hall (1999a) are numbered 1–13. Note that the monophyly of the 'hypoleuca' group is supported by the successively weighted analysis reported in Fig. 4.

Results

Cladograms

The 104 characters used in the analysis (Appendix 1) included one behavioural-ecological character, twenty-nine from wing shape and pattern, twenty from the male abdomen, thirty-three from male genitalia and twenty-one from female genitalia. Initial analysis of the dataset (Appendix 2) generated 116 500 MPCs (length = 300, CI = 0.66, RI = 0.89),

a number that represents the ceiling imposed by computer memory rather than a complete set of MPCs. The high initial number of MPCs was due to a combination of the high percentage (28%) of missing female genital data (the females of many species still remain unknown), the use of three large unordered multistate characters and a large number of taxa. Clearly, despite a common misconception to the contrary, a high number of MPCs is not necessarily indicative of low phylogenetic content in the dataset (Naylor, 1992). The strict consensus cladogram of the

Table 3. Universal synapomorphies for the species group clades of *Theope* (adapted from Hall, 1999a). The numbers 1–13 preceding each species group name refer to the same encircled numbers in Fig. 3, the numbers in parentheses after each species group name represent the number of species it contains, and the numbers in parentheses after each apomorphy refer to the character number and state in this study (see Appendix 1). Reference is given to figure numbers where appropriate.

Theope group	Synapomorphies
1 <i>nycteis</i> (3)	Submarginal spots on ventral hindwing enlarged in apex (29:1) (Fig. 2G) Last male sternite long, thin and ribbonlike with no lateral projections (50:2) (Fig. 7C)
2 <i>tetrastigma</i> (2)	Aedeagus of male genitalia possesses lightly sclerotized tissue laterally towards tip (74:1) (Fig. 11D) Aedeagus of male genitalia contains single, elongate and narrow cornutus that parallels distal edge of aedeagus when everted (79:4) (Fig. 11D)
3 <i>hypoleuca</i> (3)	None
4 <i>archimedes</i> (2)	Red scaling present at base of ventral forewing (18:1) (Fig. 2J) Thin, contrasted whitish line present along length of ventral abdominal surface (33:1) (Fig. 2J) Lower portion of uncus of male genitalia a broadly elongate triangle (57:3) (Fig. 9A) Valvae of male genitalia evenly posteriorly elongate and rounded at tip (67:7) (Fig. 10I) Dorsal portion of ostium bursae of female genitalia reduced to a sclerotized triangle in each corner (87:1) (Fig. 13G)
5 <i>pedias</i> (4)	None
6 <i>eudocia</i> (2)	Dorsal surface predominantly a uniform orange (5:2) (Fig. 1M) Valvae of male genitalia rectangular with single posteriorly projecting point from middle of distal margin (67:9) (Fig. 10K)
7 <i>sericea</i> (9)	Signa of female genitalia large and 'horn'-shaped (103:A) (Fig. 14F)
8 <i>antaniis</i> (2)	Medial white band present on both ventral surfaces (23:1) (Fig. 2O) Valvae of male genitalia narrow with basal lateral bulge of same length as remainder (67:J) (Fig. 10P)
9 <i>virgilius</i> (4)	Last male sternite 'horn'-shaped (50:7) (Fig. 7J) Medial region of vinculum of male genitalia possesses a 'hump'-like posterior projection (62:1) (Fig. 9K)
10 <i>terambus</i> (7)	Medial region of vinculum of male genitalia possesses an elongate, triangular posterior projection (62:2) (Fig. 9L) Aedeagus contains single large, arrow-shaped cornutus (78:6) (Fig. 11G) Ostium bursae of female genitalia laterally elongate and shaped like an 'open mouth' (88:1) (Fig. 12A) Signa of female genitalia very large and elongate with a broadly rounded tip (102:B) (Figs 12A, 14H)
11 <i>theritas</i> (8)	Base of forewing costa strongly bowed (2:1) (Fig. 1T) Elongate postdiscal blue on dorsal forewing of females present in cells M2 and M1 only (10:1) (Fig. 1U) Last male sternite asymmetrical (47:1) (Fig. 7K) Dorsal portion of last male sternite consists of 2 dorsoposterior projections, a very long left 'arm' and a typically shorter right 'arm' (50:A) (Fig. 7K) Lower portion of uncus of male genitalia triangular and downwardly pointed (57:1) (Fig. 9E) Falces of male genitalia angularly rectangular at base (<90°), lower edge convex, remainder long and rounded, typically with tip turned outwards (59:7) (Fig. 9E) Upper region of vinculum of male genitalia possesses an elongate posterior projection (63:1) (Fig. 9M,N) Pedicel of male genitalia asymmetrical (82:1) (Fig. 11J)
12 <i>thestias</i> (5)	Prominent yellow scaling present at base only of ventral forewing (16:1) (Fig. 2V) Last male sternite reduced to a vestigial band (50:D) (Fig. 8B) Lower portion of uncus of male genitalia a narrowly elongate triangle (57:2) (Fig. 9F) Vinculum of male genitalia forms a ventral, posterior 'cup' (66:2) (Fig. 8B) Valvae of male genitalia narrow and twisted (67:E) (Fig. 10S) Ostium bursae of female genitalia possesses 2 posteriorly concave and triangular anterolateral projections (91:1) (Fig. 13J)
13 <i>foliorum</i> (13)	Vinculum of male genitalia incomplete, extending from anterior edge of tegumen to top of valvae (60:1) (Fig. 8D) Valvae of male genitalia possess an upper posterior projection or 'arm' (67:H) (Fig. 10T,U,V)

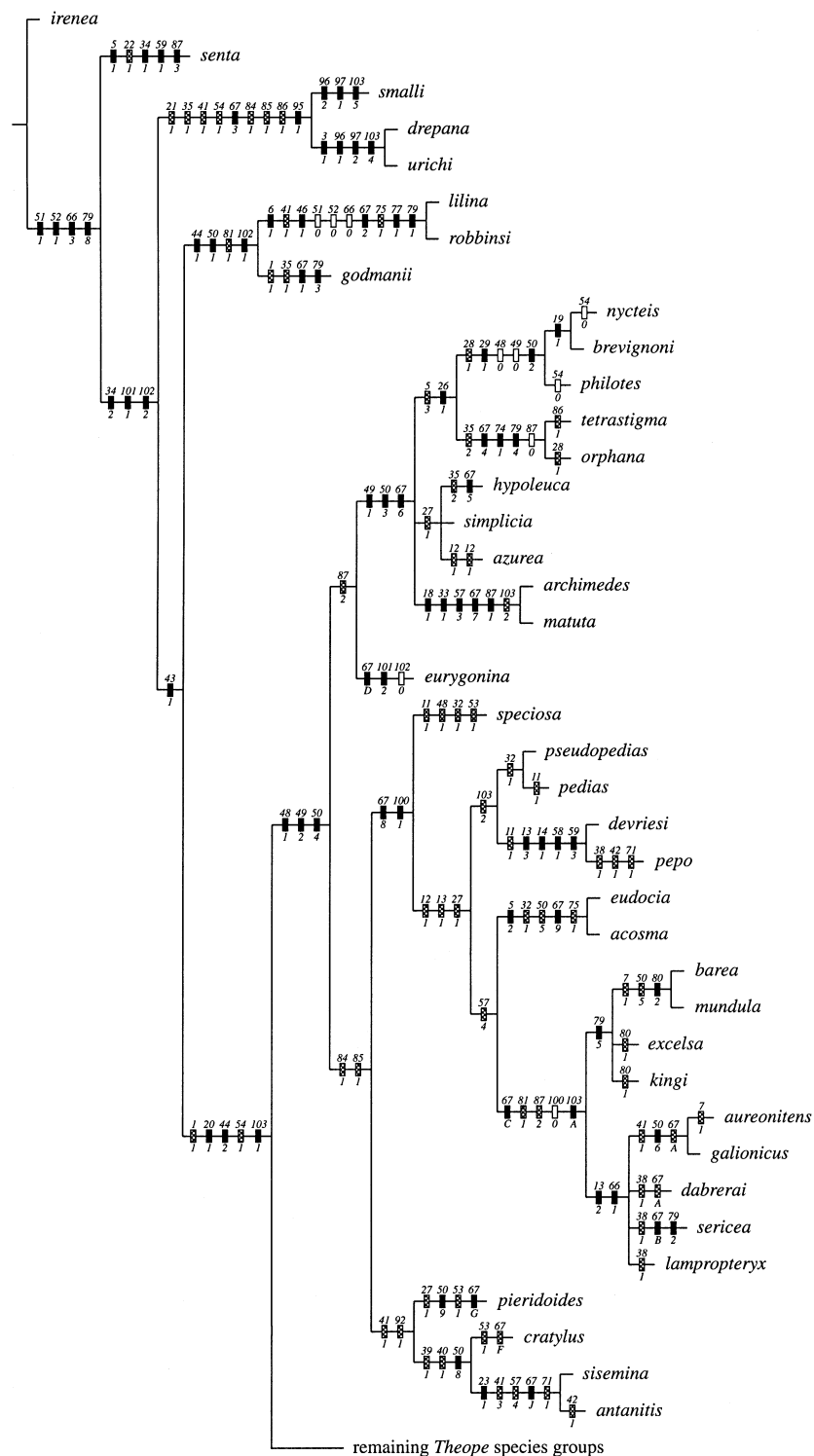


Fig. 4. Strict consensus of the final 107 644 equally parsimonious cladograms resulting from two iterations of successive approximations character weighting, illustrating *Protonymphidia*, *Archaeonymphia*, *Calicosama*, *Behemothia* and species groups 1–8 of *Theope* (remainder in Fig. 5). Black bars indicate unique apomorphies, shaded bars homoplasious apomorphies and white bars reversals.

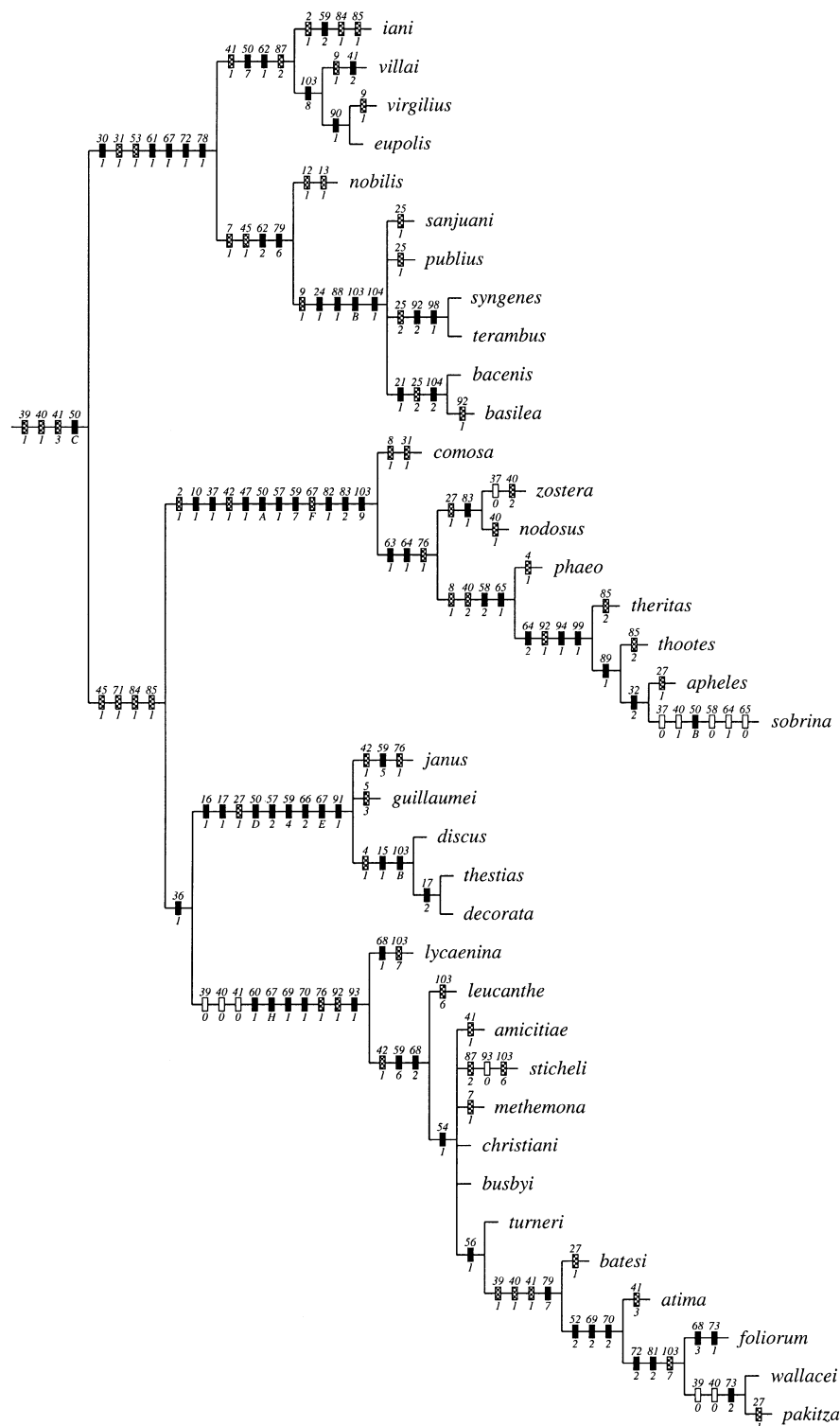


Fig. 5. Strict consensus of the final 107 644 equally parsimonious cladograms resulting from two iterations of successive approximations character weighting, illustrating species groups 9–13 of *Theope* (remainder in Fig. 4). Black bars indicate unique apomorphies, shaded bars homoplasious apomorphies and white bars reversals.

116 500 MPCs (Fig. 3) recovered all the recognized genera as monophyletic clades (or terminals) as well as all the *Theope* species groups recognized by Hall (1999a) (marked on Fig. 3 as circled numbers 1–13, and referred to in the text below) except the '*hypoleuca* group' (clade 3). The multiple heuristic searches with random addition sequences failed to find any cladograms shorter than 300 steps.

SACW resulted in the stabilization of character weights after two iterations. The strict consensus cladogram of the final 107 644 MPCs (length = 180.47, CI = 0.84, RI = 0.95) additionally recovered the '*hypoleuca* group' of *Theope*, although there is currently weak character support for its monophyly. It also produced increased resolution at deeper internal nodes, providing a more detailed, albeit weakly supported, hypothesis of relationships between *Theope* species groups. This cladogram (Figs 4, 5) is regarded as the best hypothesis of relationships within Theopeina and will form the basis of subsequent discussion.

These analyses establish the monophyly of all included genera (*Protonymphidia* and *Behemothia* are monotypic) and indicate their relationship to be *Protonymphidia* + (*Archae onympha* + ((*Calicosama* + *Behemothia*) + *Theope*)). The genera *Parnes* Westwood, [1851] (*Theope* clade 1), and *Dinoplotis* Stichel, 1911 (*orphana* Stichel, 1911; in *Theope* clade 2), are confirmed as synonymous with *Theope* (Hall, 1999a). Within the largest genus *Theope*, thirteen species group clades can be recognized. However, an additional four *Theope* species (*eurygonina* Bates, 1868; *speciosa* Godman & Salvin, 1897; *pieridoides* C. & R. Felder, 1865; and *cratylus* Godman & Salvin, 1886) typified by numerous autapomorphic characters cannot be satisfactorily grouped with any of these clades, although *pieridoides* and *cratylus* appear to be most closely related to group 8 species. Universal synapomorphies for all the generic clades/terminals and *Theope* species group clades are listed in Tables 2 and 3, respectively, and all character state changes are marked on the cladogram in Figs 4 and 5.

The high consistency indices for both final sets of MPCs, which are actually unusually high given the large number of taxa in the dataset (see Sanderson & Donoghue, 1989), are indicative of a relatively low level of homoplasy, a result that in this case has also led to high branch support for many clades. All three polytypic generic clades have bootstrap values above 85, decay indices above 3, or both, as do nine of the thirteen species group clades within *Theope*. It is generally noticeable that branch support is somewhat lower for the more basal clades within *Theope* than the more distal ones.

Morphology

In presenting an overview of character distributions and evolution in Theopeina, it is first important to mention those morphological traits not associated with the characters discussed below that were examined but not coded, and why. Antennal structure is relatively homogeneous across Papilionoidea (Hall, 1999a, provided a scanning electron

micrograph of a representative *Theope* antennal segment). As is typical for myrmecophilous species, the nudum is extensive, especially in females (Forbes, 1957; Robbins, 1991). However, this character exhibits continuous interspecific variation, as does club shape and the number of shaft segments, which I found to be directly correlated with the size of the butterfly (Hall, 1999a). The eyes of all species in Theopeina are bare and no qualitative variation could be found in the ultrastructure of the eyes and proboscis of two phylogenetically disparate species examined using the SEM. The second and particularly the third palpal segments exhibit substantial interspecific and sexual variation in length, independent of overall size of the butterfly, the third segment varying from very short in *Behemothia godmanii* (Dewitz, 1877), to very long in '*pedias* group' species of *Theope*. However, across this large dataset no suitably large gaps were observed in this variation to permit theoretically sound coding. The range of palpal variation for *Theope* was illustrated by Hall (1999a). Forelegs and midlegs were examined for eight phylogenetically disparate species in Theopeina, but no qualitative variation was found. The typical leg structures for each genus in Theopeina were figured by Hall & Harvey (1998, 2001) and Hall (1999a, 2000). Despite significant interspecific variation, the colorations of the ventral appendages (e.g. legs, palpi, etc.) were not coded because they did not vary independently from ventral wing coloration.

The use of wing venational characters in the classification of Lepidoptera has a long history (Herrich-Schäffer, 1843–1856; Comstock & Needham, 1918; Heppner, 1998), but at low taxonomic levels in Riodinidae I found such characters to be so homoplasious as to be infrequently useful for inferring phylogeny. Forewing radial venation in Theopeina is highly variable between species and the extent of fusion of veins R1 and Sc varies from none to complete, superficially reducing the number of radial veins to three. The high degree of homoplasy in this character is well demonstrated by the independent evolution of the most extreme case of fusion in two phylogenetically disparate groups of *Theope*, the '*tetrastigma*' (clade 2) and '*thestias* groups' (clade 12). In the former case, Stichel (1911) actually cited the fusion of veins R1 and Sc as the predominant reason for describing the synonymous genus *Dinoplotis* (Hall, 1999a). Irrespective of the homoplasy inherent in this character, it was too continuously variable to be able to code.

Wing shape and pattern. Wing pattern characters are often purposely omitted from cladistic analyses due to concerns about homology (e.g. DeVries *et al.*, 1985). In general, it is certainly true that the evolutionary processes of sexual and natural selection, particularly when resulting in selection for mimicry (Vane-Wright & Smith, 1991; Brower, 1994; Miller, 1996), can lead to extensive wing pattern convergence, but at relatively low taxonomic levels where mimicry is not a factor, as in this study, wing pattern characters can provide valuable phylogenetic information. Indeed, although the three main character sets of wing pattern, male and female genitalia all have similar CIs, the wing pattern character set actually has the highest CI.

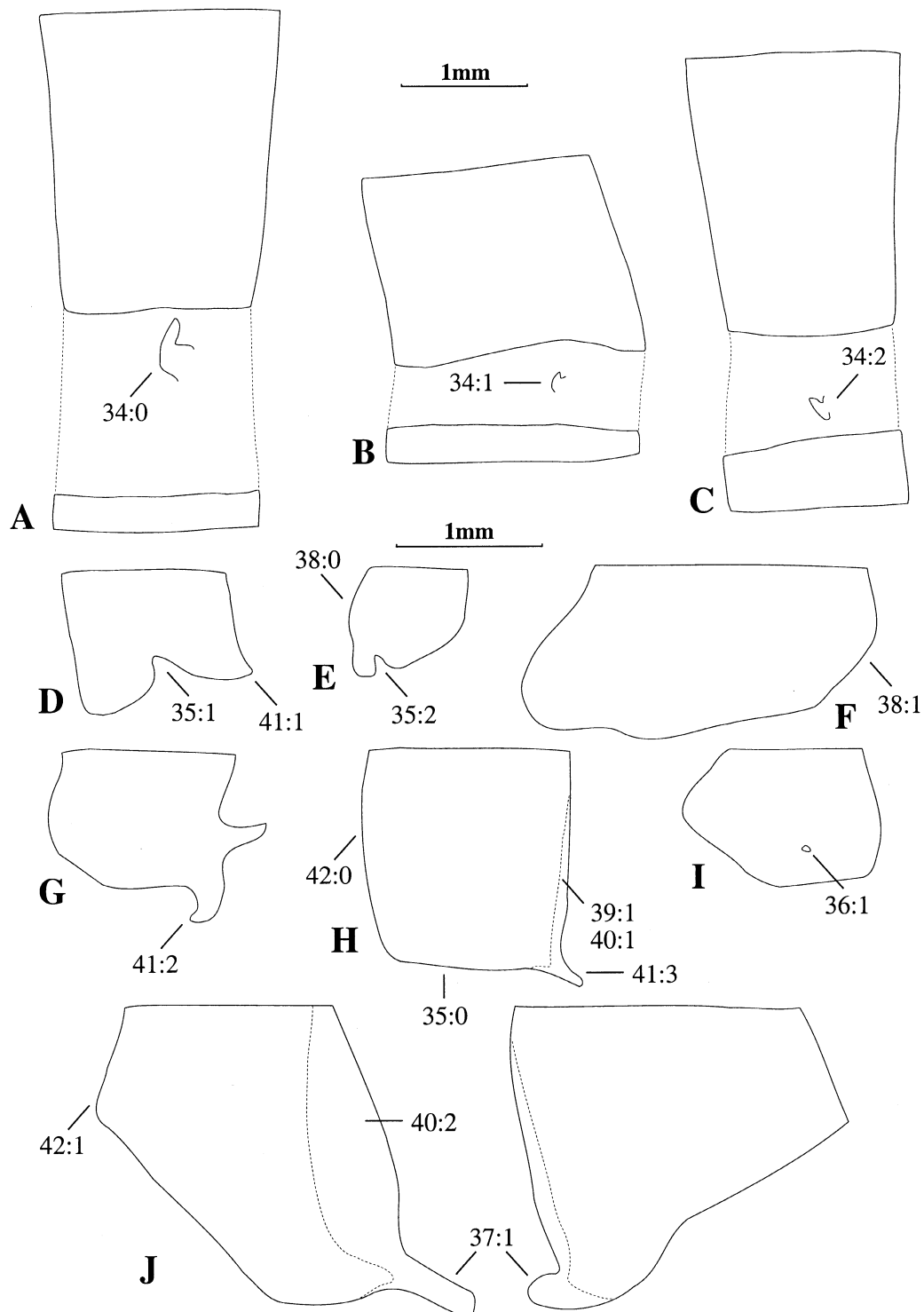


Fig. 6. Representative male abdominal sclerites for Theopeina, illustrating characters 34–42 in Appendix 1. A–C represent the spiracle position on abdominal segment three for the following species: A, *Thisbe irenea*; B, *Protonymphidia senta*; C, *Theope lampropteryx*. D–J represent the last (eighth) tergite in lateral view (on both sides of the abdomen for J) for the following species: D, *Archaeonympha drepana*; E, *Theope tetrastigma*; F, *Theope sericea*; G, *Theope villai* (adapted from Beutelspacher, 1981); H, *Theope basilea*; I, *Theope methemona*; J, *Theope theritas*.

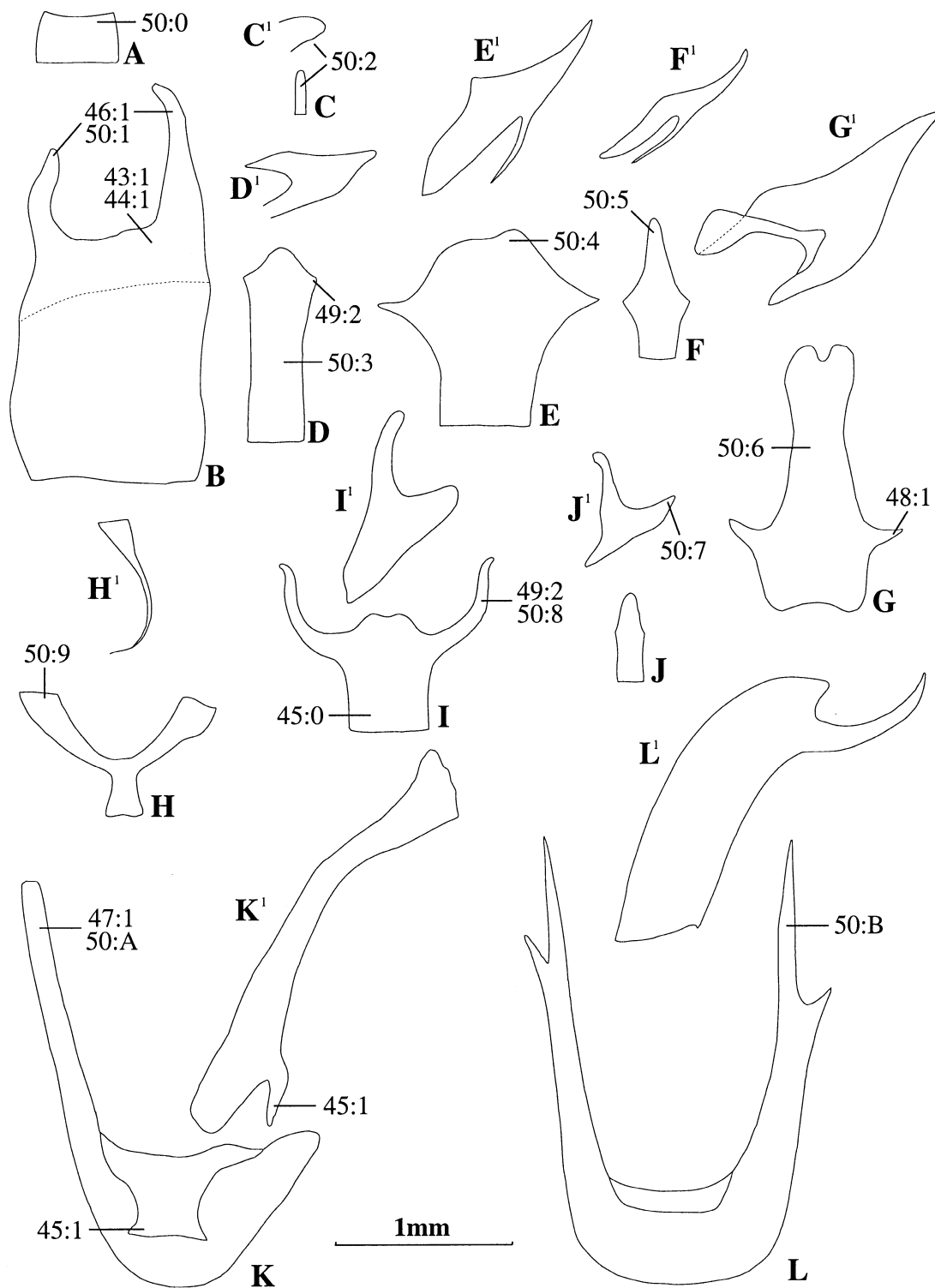


Fig. 7. Representative last (eighth) male abdominal sternites for Theopeina, illustrating characters 43–50 in Appendix 1. All sternites are figured in ventral view, but those in C–L are also figured in lateral view (marked with a superscript 1). A, *Archaeonympha drepana*; B, *Calicosama lilina*; C, *Theope nycteis*; D, *Theope archimedes archimedes*; E, *Theope pepo*; F, *Theope eudocia*; G, *Theope galionicus*; H, *Theope pieridoides*; I, *Theope antanitis*; J, *Theope virgilius*; K, *Theope nodosus*; L, *Theope sobrina*.

Overall, wing pattern characters tend to provide corroborating evidence for the monophyly of clades delineated by genital characters, but they only provide universal synapomorphies for six of the thirteen species groups within *Theope*. The most obvious trend in wing pattern evolution of *Theopeina* is the gradual reduction in ventral wing markings (see Fig. 2), and the complete lack of any ventral markings on many species of the most derived genus, *Theope*, is one of the most characteristic external features of that genus. This evolutionary pattern has provided one of only two universal synapomorphies for *Theope* (see Table 2), the total absence of spots or rare presence of a single spot (*T. eurygonina* only) instead of two at the base of cell Cu2 on the ventral forewing (ch. 20) (Fig. 2) (Hall, 1999a). This loss also occurs several times in Nymphidiina, in the genera *Setabis* Westwood, [1851], *Pandemos* Hübner, [1819], and *Zelotea* Bates (1868) (e.g. see d'Abrera, 1994). However, a uniformly coloured, patternless ventral surface is unique within Riodinidae to *Theope*, as are the gaudy orange ('*pedias* group', clade 5) and yellow ('*eudocia*' and '*sericea* groups', clades 6 and 7) ventral colours of many species (see Fig. 2K–N).

Possibly one of the most unusual ventral wing patterns of *Theopeina* occurs in species of the basal '*nycteis* group' of *Theope* (clade 1), which exhibit fine-grained, undulating yellow banding (ch. 19), termed a 'ripple pattern' by Nijhout (1991) (see Fig. 2G). This pattern is found nowhere else in Riodinidae, although it is common in the nymphalid subfamilies Satyrinae and Brassolinae. It is the main reason why '*nycteis* group' species were treated in the separate genus *Parnes* until recently (Hall, 1999a). It is only through cladistic analyses that this wing pattern has been hypothesized to have evolved from a typical *Theope*-like ancestor, probably a species similar to *T. tetrastigma* Bates, 1868 (clade 2) (Figs 1H, 2H).

Male androconia form another set of external morphological traits documented in *Theopeina*, but only rarely elsewhere in Nymphidiini. The physiological function of many scale types is still uncertain (Downey & Allyn, 1975; Scoble, 1992), but many *Theope* species possess what appear to be androconial scales in the postdiscal area of the dorsal forewing (ch. 7) (Fig. 2N,R,S). Yet others possess more highly modified androconial scales dorsally on certain segments of the abdomen (ch. 32) (Fig. 2M,T) (see Hall, 1999a, for SEMs). Because wing androconia occur in three disparate species groups, the '*sericea*', '*terambus*' and '*foliorum* groups' (clades 7, 10 and 13), and external abdominal androconia occur in two other disparate groups (three species groups), the '*pedias* + *eudocia*' and '*theritas* groups' (clades 5, 6 and 11), it is clear that such organs are repeatedly selected for.

Male genitalia and abdomen. As outlined in the introduction, Harvey (1987) used a ventral (Fig. 6C), rather than dorsal (Fig. 6A), position of the spiracle on abdominal segment 3 of males to define Nymphidiini, a character state that is found in both adults and larvae (Harvey, 1987). Although there are several basal genera in subtribe Nymphidiina that actually possess a medially positioned spiracle

(ch. 34) (Fig. 6B) (Hall, unpublished data), the only taxon to possess this character state in *Theopeina* is its apparently most basal taxon, *Protonymphidia senta*. The shape of the spiracle is interspecifically highly variable, as is its exact position, which was measured with respect to the two sclerites for each species. However, discrete variation could not be delineated for either character.

The elaborate modifications of the terminal (eighth) sclerites (Figs 6, 7) in members of *Theopeina* are unparalleled in Riodinidae. They are especially varied and ubiquitous in *Theope*, where their exact form provides excellent clues to species group membership. Such structures occur sporadically throughout Lepidoptera, and their function appears to be to aid in clasping the female abdomen during copulation, in conjunction with the valvae (Miller, 1988, 1996). Posterior projections from the last tergite (ch. 41) are found nowhere else in the family but in *Theope* (Fig. 6G,H,J), although not all species possess them. Such projections occur only in the distal half of the genus, from clade 8 onwards, although they are subsequently lost in most species of the '*foliorum* group' (clade 13). Interestingly, in conjunction with several genital asymmetries in both sexes, the entire shape of the last tergite in members of the '*theritas* group' (clade 11) is asymmetrical (ch. 37) (Fig. 6J). The strongest evidence for the sister-group relationship of the two most distal groups in *Theopeina*, the '*thesias*' and '*foliorum* groups' of *Theope* (clades 12 and 13), comes from the presence of a tiny, lightly sclerotized fenestration towards the ventral margin of the last tergite (ch. 36) (Fig. 6I), which, as in the invaginations along the ventral margin in certain basal groups (ch. 35) (Fig. 6D,E), is probably spiracular in origin.

The second, and in this instance unique, universal synapomorphy for *Theope* (see Table 2) is found in the terminal (eighth) sternite of males, which has a sclerotized invagination dorsally that extends to connect to the base of the genital armature (ch. 44) (Fig. 8A) (Hall, 1999a), to which it is typically attached when the genitalia are dissected out of the abdomen. It is presumably for this reason that Penz & DeVries (1999) erroneously reported *Theope virgilius* (Fabricius, 1793) and *T. publius* C. & R. Felder, 1861, as possessing only seven abdominal sternites (consequently regard the eighth sternite as fused valvae). Dorsal sclerotized invaginations do occur in a few basal species of *Theopeina* (e.g. see Fig. 7B) and a few species of Nymphidiina, but these are restricted to the posterior half of the sternite and connected to the genital armature only by extensive membranous tissue. The shape of the last sternite also provides apomorphies for *Calicosama* and *Behemothia* (ch. 50). The main evolutionary trend in terminal sternite structure throughout the large genus *Theope* is the gradual reduction in the ventral element from the typical rectangular shape of most riodinid ventral sclerites in the basal half of the genus (clades 1–8) (Fig. 7A), to a tiny vestigial triangle or band in the most distal species groups (clades 10–13) (Figs 7K, 8B,D). Paradoxically, however, there is a concomitant increase in overall structural complexity in the same direction, at least as far as the

'theritas group' (clade 11), from the simple ribbonlike terminal sternite of the 'nycteis group' (clade 1) (Fig. 7C) to the enormous three-dimensional structures of certain 'sericea group' species (clade 7) (Fig. 7G), and the elongate dorsolateral projections of the 'sisemina group' (clade 8) (Fig. 7I) (ch. 50). The most bizarre terminal sternite modi-

fications are to be found in the 'theritas group' of *Theope* (clade 11), in which the dorsal element is asymmetrically produced into a very long left projection and a typically much shorter right projection (ch. 47) (see Fig. 7K,L). One species in this group, *Theope sobrina* Bates, 1868, possesses perhaps the most formidable array of what are

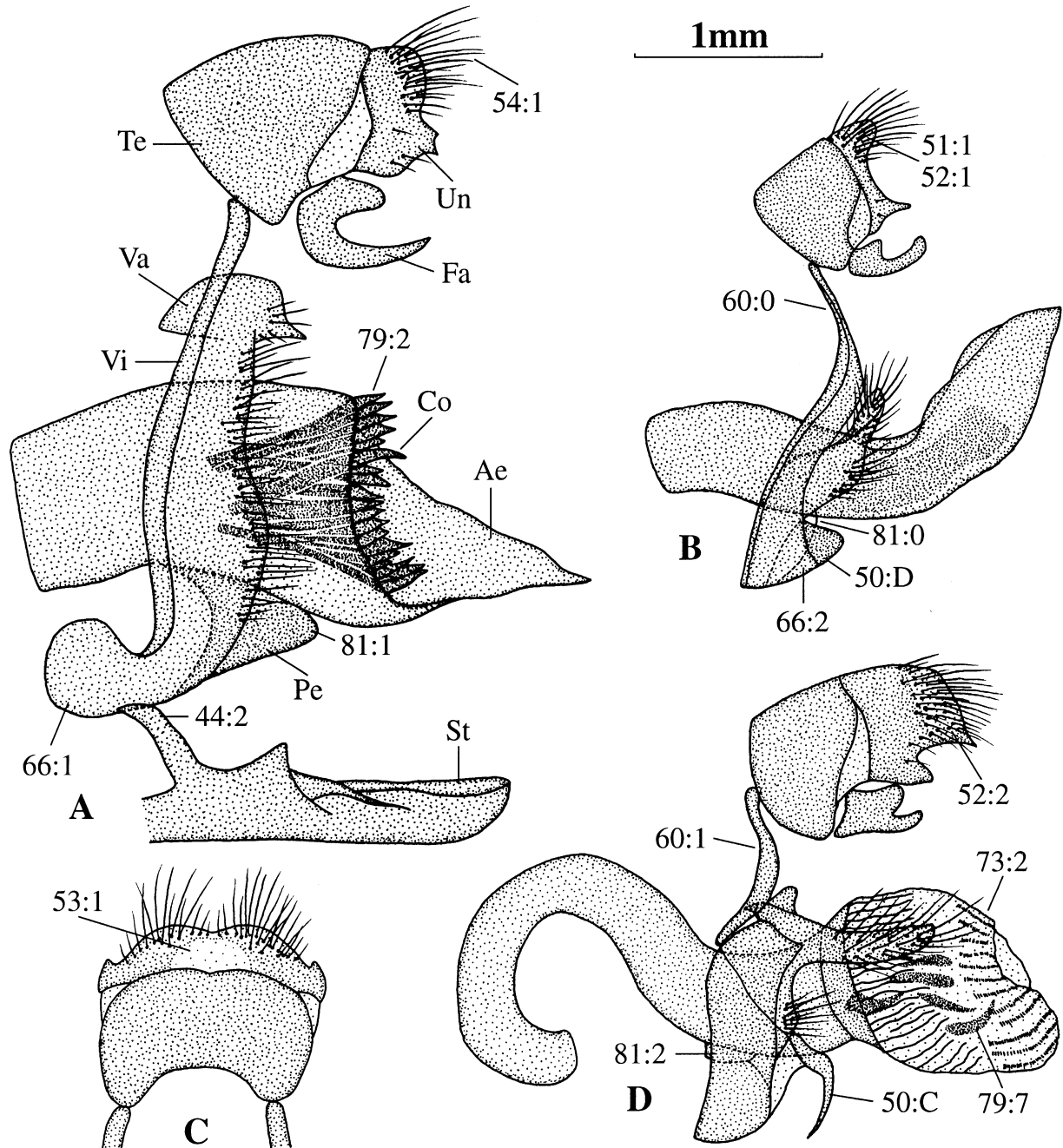


Fig. 8. Selected male genitalia of *Theopeina*, illustrating characters 44, 50–54, 60, 66, 73, 79 and 81 in Appendix 1. C represents an uncus in dorsal view, the remainder represent the entire genital armature, with eighth sternite attached, in lateral view. A, *Theope sericea*; B, *Theope thestias*; C, *Theope virgilius*; D, *Theope wallacei*. Abbreviations on A: Te = tegumen; Un = uncus; Fa = falcis; Vi = vinculum; Va = valva; Ae = aedeagus; Co = cornutus; Pe = pedicel; St = eighth sternite.

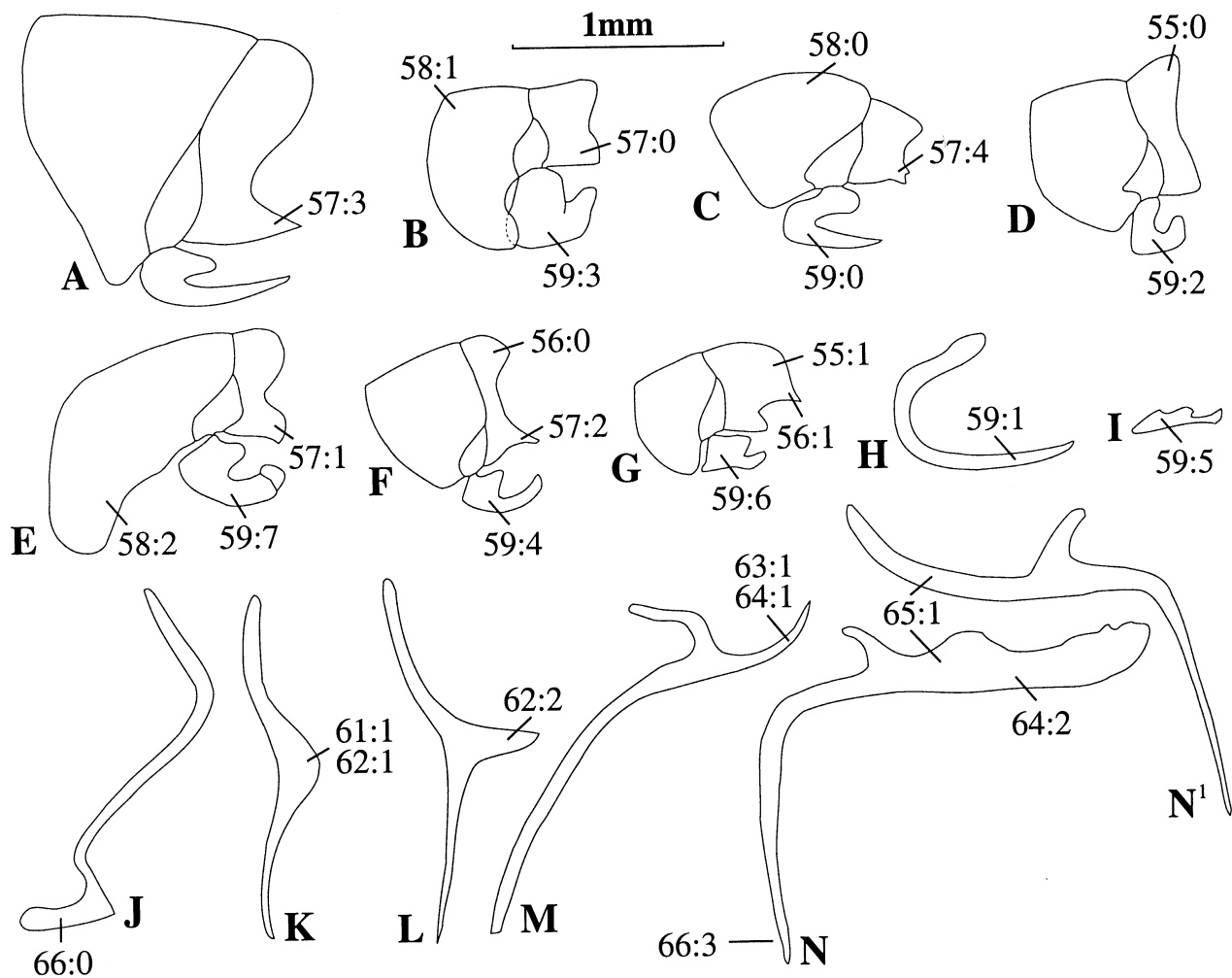


Fig. 9. Representative male genital uncus (A–G), falces (A–I) and vincula (J–N) for *Theopeina*, illustrating characters 55–65 in Appendix 1. All structures are figured in lateral view and those in N in left and right lateral views (marked with a superscript 1). A, *Theope matuta heureka*; B, *Theope pepo*; C, *Theope dabrerai*; D, *Theope iani*; E, *Theope thootes*; F, *Theope discus*; G, *Theope wallacei*; H, *Protonymphidia senta*; I, *Theope janus*; J, *Thisbe irenea* (outgroup taxon); K, *Theope eupolis*; L, *Theope publius publius*; M, *Theope sobrina*; N, *Theope thootes*.

presumably copulatory grappling structures in all Riodinidae, including a small blunt posterior projection from the last tergite, and elongate, spiky posterior projections from the highly modified last sternite (Fig. 7L), the valvae and vinculum (Fig. 9M) (see below).

Since the turn of the nineteenth century (e.g. Godman & Salvin, 1879–1901), male genitalia have been the most widely used morphological structures in lepidopteran classification at middle and low taxonomic levels. In *Theopeina*, the shapes of the uncus (chs 51–57), falces (ch. 59), vincula (chs 60–66) (Fig. 9), aedeagi and internal cornuti (chs 71–80) (Fig. 11), and particularly the valvae (chs 67–70) (Fig. 10), provide a wealth of characters that allow the delimitation of species groups and the separation of otherwise superficially similar species. For example, species that have long been confounded with each other, such as *Theope lycaenina* Bates, 1868 (Fig. 1X), and *Theope wallacei* Hall, 1998 (Fig. 1Y), have distinctive genitalia that place them in

different subgroups of the ‘*foliorum* group’ (clade 13) (Figs 8D, 10T). This is in stark contrast to subtribe *Nymphidiina*, the members of which (particularly the distal ones) exhibit an equally remarkable homogeneity in male genitalia (Hall, unpublished data). The valvae, as their common name ‘claspers’ suggests, are typically the predominant clasping structures utilized during copulation, and those of, for example, the ‘*foliorum* group’ of *Theope* (clade 13) (Fig. 10U,V) appear to be particularly well adapted to this function. However, as well as having terminal sclerites and valvae evolved for copulatory clasping, certain members of *Theope*, particularly those in the ‘*terambus*’ and ‘*theritas* groups’ (clades 10 and 11), are extraordinary in possessing variably elongate posterior projections from the upper half of the vinculum (chs 61–64) (Fig. 9K–N) that have presumably evolved for the same purpose. It is a character that is seen only rarely elsewhere in the family (e.g. in the symmachiine genus *Pirascia* Hall & Willmott, 1996).

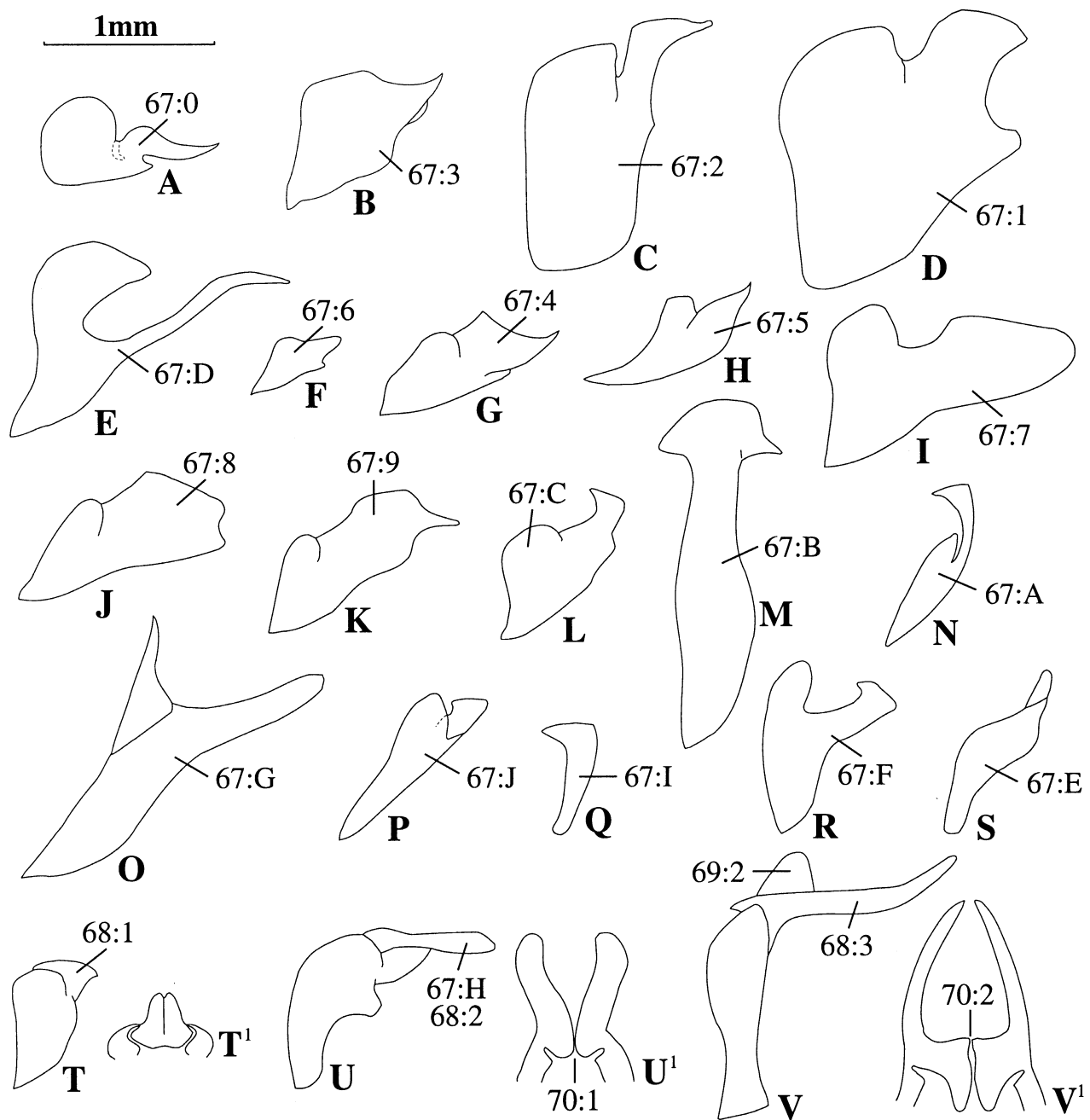


Fig. 10. Representative male genital valvae for Theopeina, illustrating characters 67–70 in Appendix 1. All structures are figured in lateral view, but those in T–V are also figured in dorsal view (marked with a superscript 1). A, *Protonymphidia senta*; B, *Archaeonympha drepana*; C, *Calicosama lilina*; D, *Behemothia godmanii*; E, *Theope eurygonina*; F, *Theope brevignoni*; G, *Theope orphana*; H, *Theope hypoleuca*; I, *Theope archimedes archimedes*; J, *Theope devriesi*; K, *Theope eudocia*; L, *Theope mundula*; M, *Theope sericea*; N, *Theope dabrerai*; O, *Theope pieridoides*; P, *Theope sisemina sisemina*; Q, *Theope publius publius*; R, *Theope nodosus*; S, *Theope thestias*; T, *Theope lycaenina*; U, *Theope turneri*; V, *Theope foliorum*.

Female genitalia and abdomen. The terminal tergite of the female abdomen exhibits minimal variation compared to that of the male, but a ‘disc’ at the upper posterior corner does vary in its degree of sclerotization (ch. 84), and in certain members of the ‘*theritas* group’ of *Theope*

(clade 11) its posterior length is also variable (ch. 85) (Fig. 13A,B). Characters of the female genitalia have historically been under-utilized in lepidopteran systematics compared with those of the male, and in fact the first riodinid classification to encompass them was that of

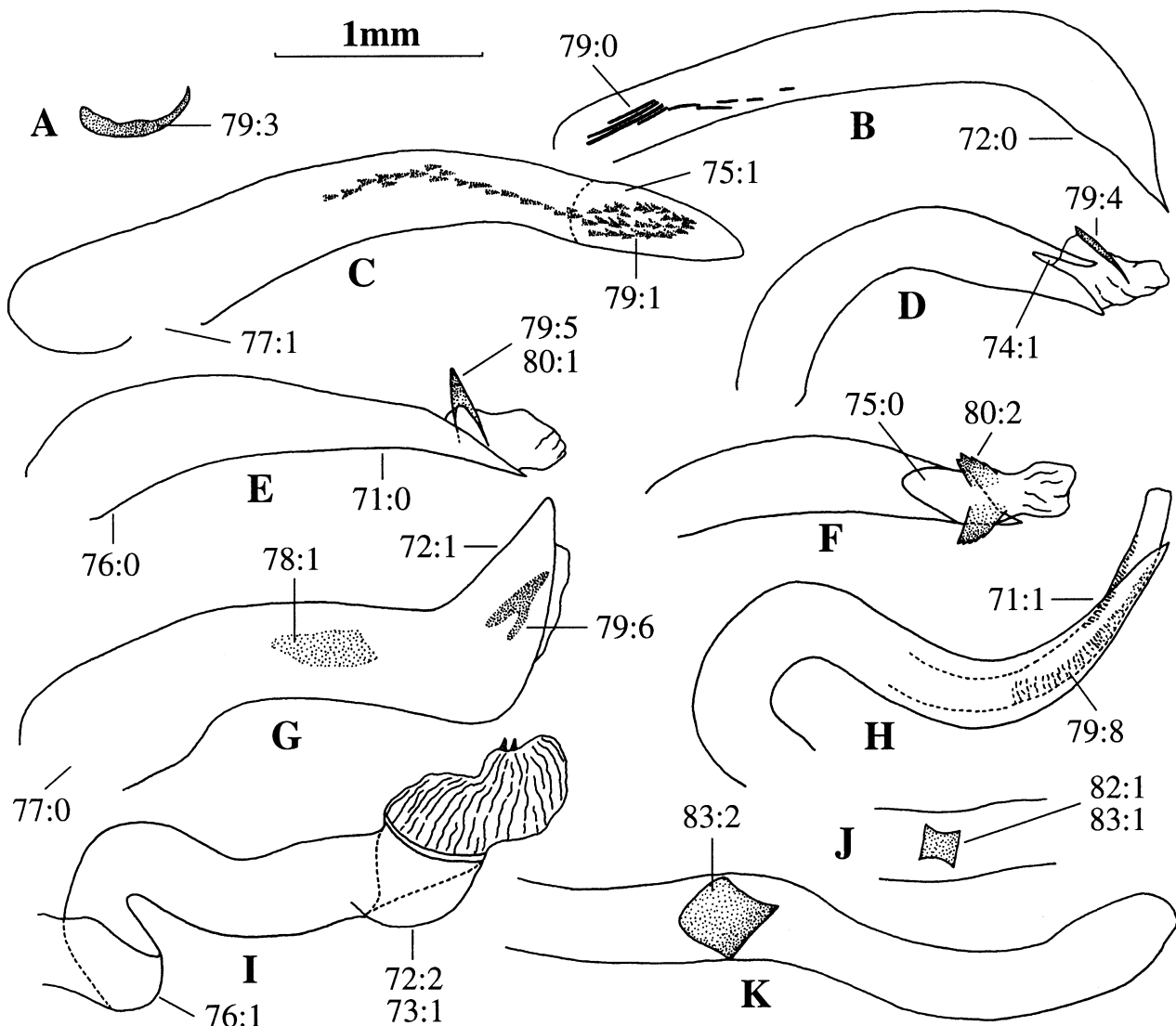


Fig. 11. Representative male genital aedeagi and cornuti for Theopeina, illustrating characters 71–80 and 82–83 in Appendix 1. A (single cornutus) is illustrated in dorsal view, B–I (aedeagi with cornuti) in lateral views and J–K (aedeagi with pedicels) in ventral view. A, *Behemothia godmanii*; B, *Thisbe irenea* (outgroup taxon); C, *Calicosama lilina*; D, *Theope orphana*; E, *Theope excelsa*; F, *Theope mundula*; G, *Theope virgilius*; H, *Theope leucanthæ*; I, *Theope foliorum*; J, *Theope thootes*; K, *Theope zostera*.

Harvey (1987). This study represents the most extensive review of female genitalia for any single large group of riodinids to date. In Theopeina, female genitalia are more evolutionarily conservative than those of the male and because they are less structurally complex they exhibit less variation. However, the shape of the ostia bursarum (chs 87–91) (Figs 12, 13) and signa (chs 101–104) (Fig. 14), and the degree of sclerotization in and shape of the ducta bursae and seminalis (chs 92–100) (Fig. 12), still provide many species group characters, and, importantly, phylogenetic information at levels above the species group. Indeed, the presence of an elongate, hollow sclerotized structure in the middle of the ductus bursae at the opening to the ductus seminalis (ch. 95) (Fig. 13C,D) is a unique

universal synapomorphy for *Archaeonympha* (see Table 2) (Hall & Harvey, 1998). No variation could be found in the shape of the papillae anales, and, although some variation occurs in the shape of the corpus bursae, this could not be coded. Anteriorly directed spines on the inner surface of the corpus bursae, as reported by Robbins (1991) for the eumaeine lycaenid genus *Rekoa* Kaye, were observed in two *Theope* species and found to vary in shape and spacing (Hall, 1999a). Although these characters might provide useful phylogenetic information, it was beyond the scope of this study to examine the corpus bursae of all species using scanning electron microscopy.

Several broad evolutionary patterns in the group are worthy of mention. The ostium bursae is typically sclerotized

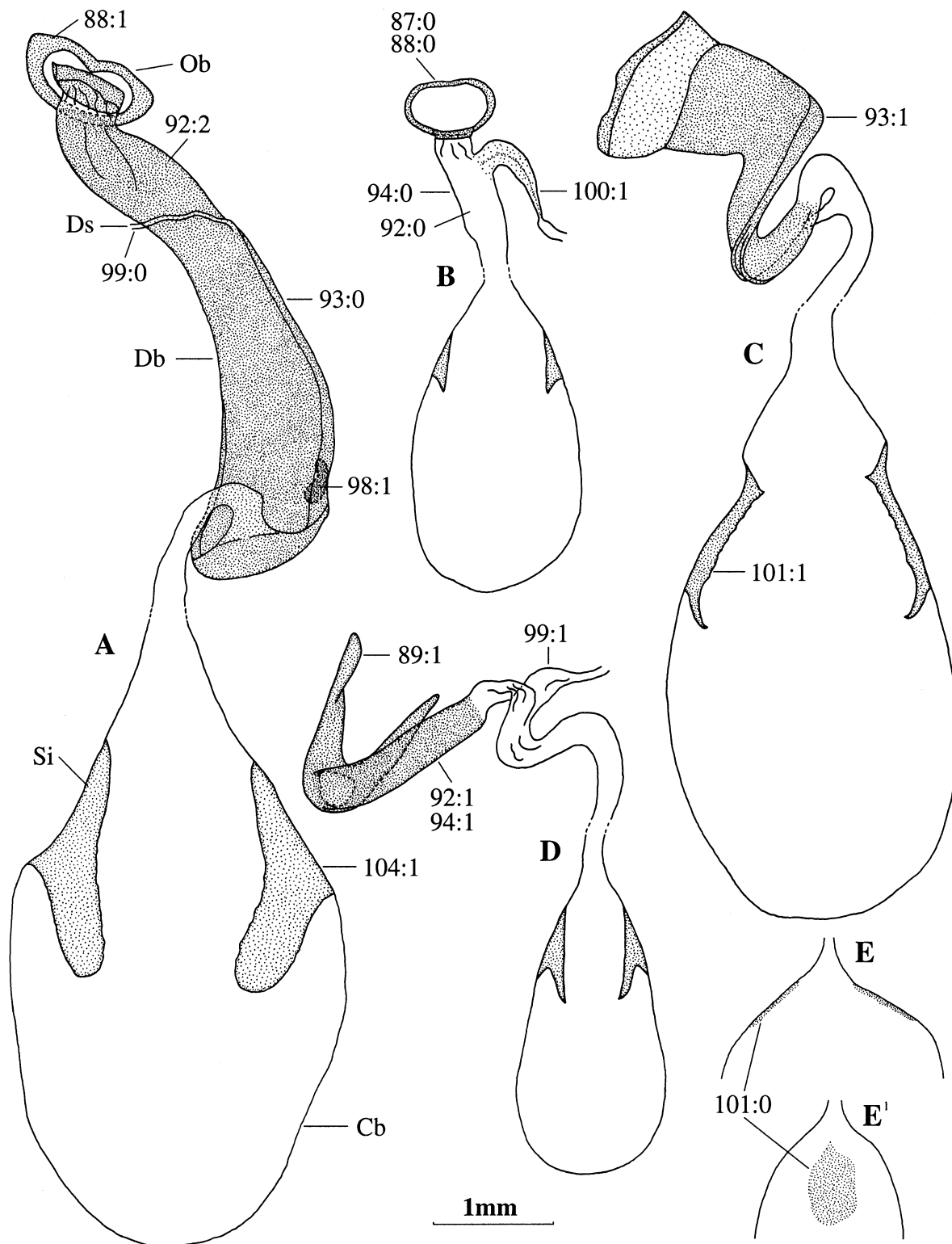


Fig. 12. Selected female genitalia of *Theopeina*, illustrating characters 87–89, 92–94 and 99–101 in Appendix 1. A–D represent all copulatory organs of the genitalia, and E represents the posterior end of the corpus bursae in dorsal and lateral views (marked with a superscript 1). A, *Theope terambus*; B, *Theope devriesi*; C, *Theope wallacei*; D, *Theope apheles*; E, *Protonymphidia senta*. Abbreviations on A: Ob = ostium bursae; Db = ductus bursae; Ds = ductus seminalis; Cb = corpus bursae; Si = signum.

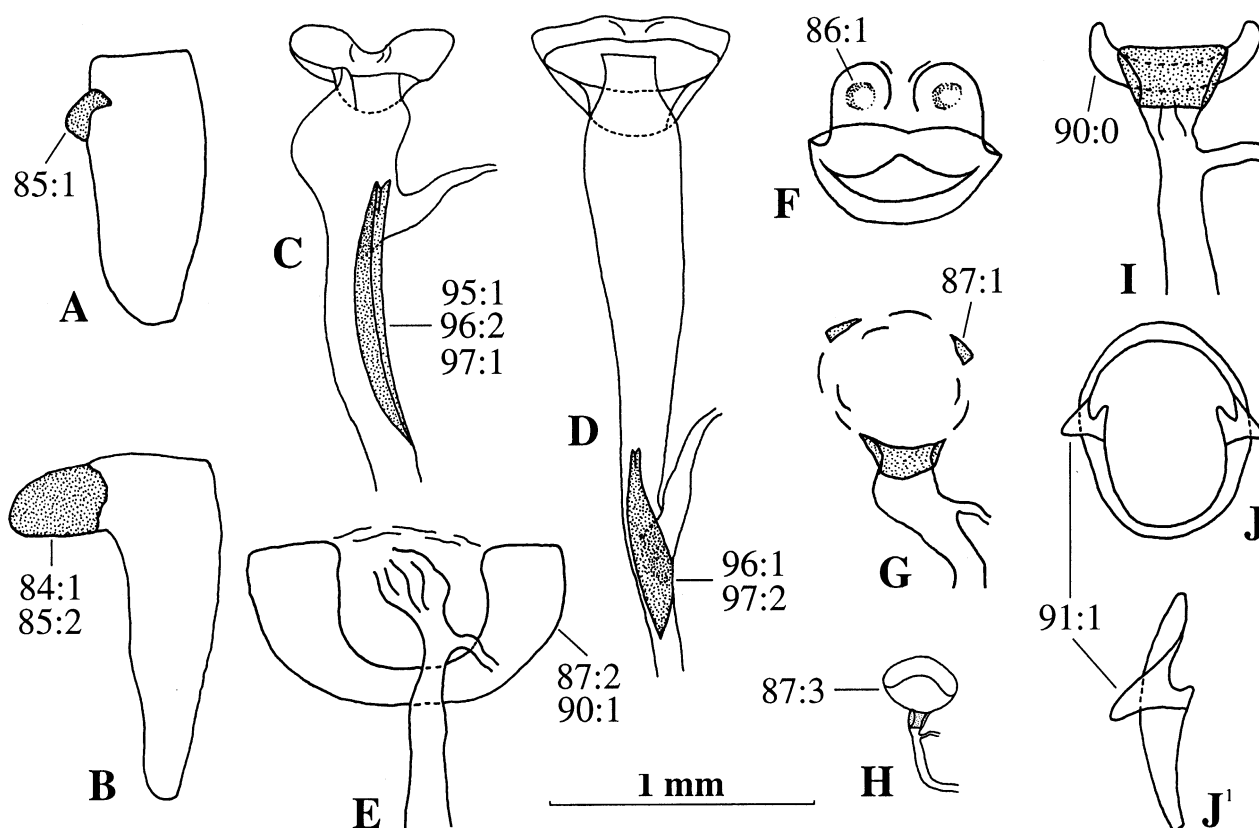


Fig. 13. Representative last (eighth) female abdominal tergites (A,B) and posterior female genital structures (C–J, ostium and ductus bursae) for Theopeina, illustrating characters 84–87, 90–91 and 95–97 in Appendix 1. A,B are figured in lateral view, C–E and G–I in dorsal view, J in ventral and lateral view (marked with a superscript 1) and F in ventral view. A, *Theope apheles*; B, *Theope thootes*; C, *Archaeonympha smalli*; D, *Archaeonympha drepana*; E, *Theope virgilius*; F, *Theope tetrastigma*; G, *Theope archimedes archimedes*; H, *Protonymphidia senta*; I, *Theope kingi*; J, *Theope discus*.

only ventrally in the most basal groups. However, it becomes a heavily sclerotized ring in most of the distal groups (ch. 87) (Figs 12, 13), where the shape often becomes more elaborate (ch. 91) (Fig. 13J), as notably in the 'theistias group' of *Theope* (clade 12). The degree of sclerotization in the posterior half of the ductus bursae (ch. 92) also increases markedly in the same direction, with heavily sclerotized tubes being prevalent in most members of the 'terambus', 'theritas' and 'foliorum' groups of *Theope* (clades 10, 11 and 13) (Fig. 12). A character state that is known to occur elsewhere in Riodinidae only in *Charis* (Hall & Harvey, unpublished data) is the coiling of this sclerotized tube (posterior half of ductus bursae) in the 'foliorum group' (clade 13) (ch. 93) (Fig. 12C), which appears to be correlated to a degree with the contorted shape of the male aedeagus (chs 71 and 76). Also of note is that in most riodinid species the ductus seminalis is a narrow very lightly sclerotized tube, but in the 'pedias' and 'eudocia' groups of *Theope* (clades 5 and 6), it is very broad and hardened as it joins to the ductus bursae (ch. 100) (Fig. 12B).

Discussion

This study represents the first comprehensive species-level phylogenetic analysis for any large group of Riodinidae, and as such forms the first step towards delineating units within the family. Subtribe Theopeina exhibits perhaps the greatest range of morphological variation for any group of its size in the family, predominantly between species groups, and thus a wealth of characters were available for phylogenetic study. Although there is often morphological homogeneity within groups, especially the most derived ones, indicative of recent species radiation, the group is clearly ancient, and based on evidence from Dominican amber, at least 15 or 20 million years old (Iturralde-Vinent & MacPhee, 1996; DeVries & Poinar, 1997). Given the large character set and the high degree of character and branch support for most of the labelled clades, the cladograms in Figs 3–5 must be regarded as reasonably robust hypotheses of phylogenetic relationships within the group. However, the support for and resolution of certain clades still remains unsatisfactory. The inclusion of early stage characters,

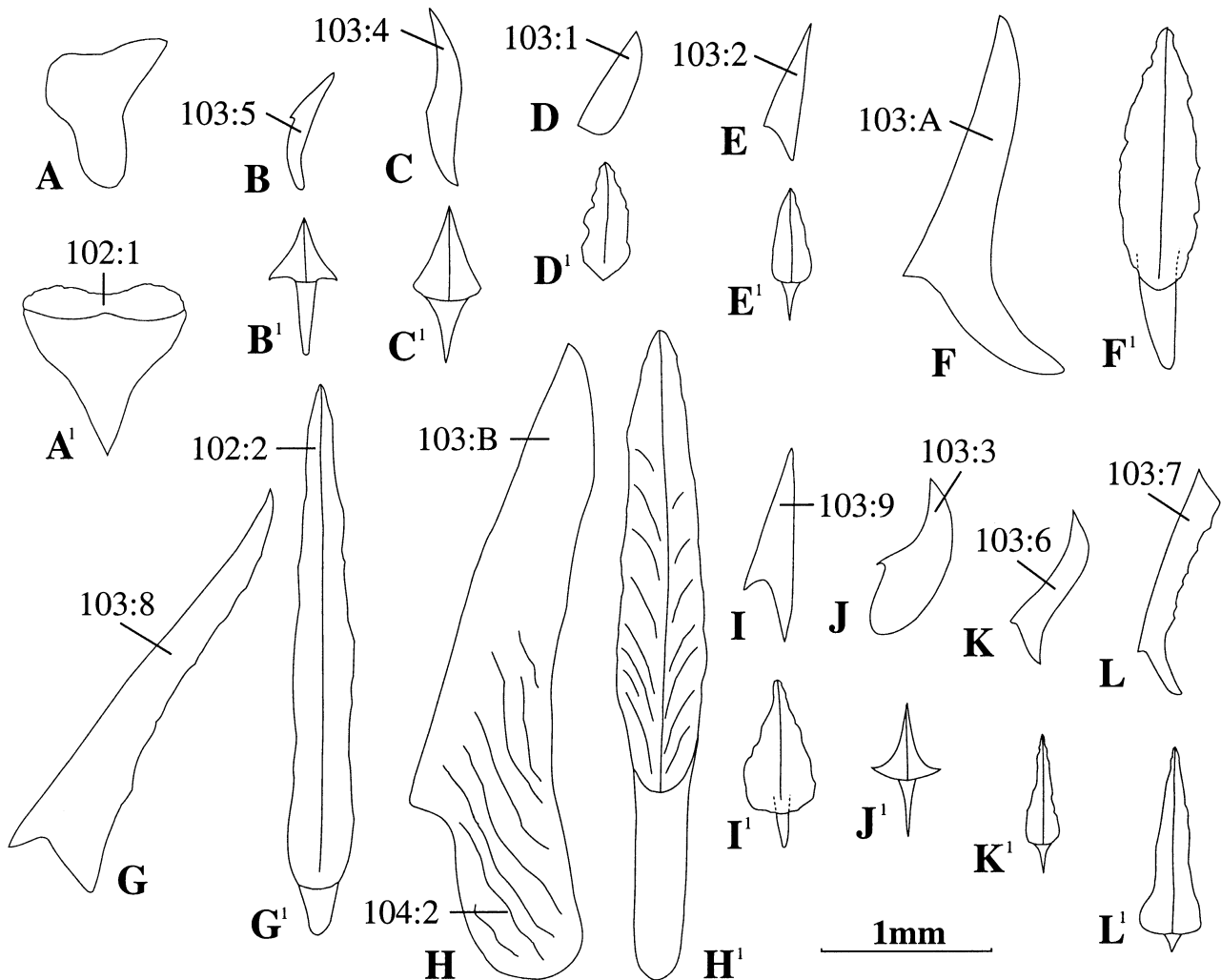


Fig. 14. Representative female genital signa for Theopeina, illustrating characters 102–104 in Appendix 1. All signa are figured in lateral and dorsal view (marked with a superscript 1). A, *Behemothia godmanii*; B, *Archaeonympha smalli*; C, *Archaeonympha urichi*; D, *Theope cratylus*; E, *Theope devriesi*; F, *Theope kingi*; G, *Theope virgilius*; H, *Theope basilea*; I, *Theope comosa*; J, *Theope discus*; K, *Theope leucanthé*; L, *Theope lycaenina*.

if and when they become available, might aid in providing better support for deeper nodes (Alexander, 1990; Miller, 1991, 1996), and molecular data might be especially helpful in resolving sibling species complexes in the most recent lineages (Miller *et al.*, 1997). The most prominently unresolved portion of the cladogram lies in the 'foliorum group' of *Theope* (clade 13), due largely to the high percentage of unknown females in the group. However, as the genitalia of known females exhibit considerable variation, it is likely that when these unknown females are discovered, their character information will substantially help to resolve relationships within this distal clade. The exact placement on the cladogram of the four species that do not fall clearly into any species group, particularly *eurygonina*, also remains somewhat uncertain and only the use of additional character sets is likely to resolve this problem.

As a result of this phylogenetic study, a number of changes in the classification of this group were required. At the outset, only three generic names were nomenclaturally available for the species included here in Theopeina, but two of those, *Parnes* (clade 1) and *Dinoplotis* (part of clade 2), needed to be synonymized with the third, *Theope* (Hall, 1999a). It was thus necessary to provide names for the remaining four generic clades/terminals highlighted in this study, namely *Archaeonympha* (Hall & Harvey, 1998), *Calicosama* (Hall & Harvey, 2001) and *Protonymphidia* and *Behemothia* (Hall, 2000). Prior to this study, the members of these last three genera were treated in the then polyphyletic genera *Calociasma* Stichel, 1910, *Adelotypa* Warren, 1895, and *Pandemos* Hübner, [1819], respectively (e.g. see Bridges, 1994), genera now treated as belonging in Nymphidiina (Hall & Harvey, 1998, 2001; Hall, 1999a, 2000).

Acknowledgements

I am greatly indebted to the primary financial supporters of my field work in Ecuador, which led to the discovery of several new *Theope* species: in 1993, an Oxford–Cambridge University expedition was supported by numerous people and institutions including Oxford University (Poulton Fund), Christ's College Cambridge University and The Royal Entomological Society; in 1995 and 1996, grants were gratefully received from Sigma Xi, the Scientific Research Society & Equafor (1996); and in 1997–2000, the National Geographic Society fully funded my fieldwork and museum research with an Exploration and Research Grant (# 5751–96). I thank the Pontificia Universidad Católica, the Museo Nacional de Ciencias Naturales and INEFAN in Quito for arranging the necessary permits for research in Ecuador. I thank those who gave me access to the riodinid collections in their care: Phillip Ackery, The Natural History Museum, London; George Austin, Nevada State Museum, Nevada; Robert and George Busby, Boston, Massachusetts; Philip DeVries, Eugene, Oregon; Donald Harvey and Robert Robbins, National Museum of Natural History, Smithsonian Institution, Washington, DC; John Heppner, Florida State Collection of Arthropods, Division of Plant Industry, Gainesville, Florida; Lee and Jacqueline Miller, Allyn Museum of Entomology, Florida Museum of Natural History, Sarasota, Florida; James Miller and Fred Rindge, American Museum of Natural History, New York; Wolfram Mey and Matthias Nuß, Zoologische Museum für Naturkunde, Humboldt Universität, Berlin, Germany; Philip Perkins, Museum of Comparative Zoology, Harvard University, Cambridge, Massachusetts; and Jacques Pierre, Musée Nationale d'Histoire Naturelle, Paris, France. The curators of all these collections kindly allowed me to photograph and borrow abdomens or specimens, and for their time, help and enthusiastic support I am most grateful. I thank Donald Harvey for stimulating discussion on riodinid systematics and comments on the character list, and Thomas Emmel, John Heppner, James Lloyd, Jon Reiskind, Robert Robbins, Richard Vane-Wright, Keith Willmott and two anonymous reviewers for critical comments on all or parts of the manuscript.

References

- d'Abrera, B. (1994) *Butterflies of the Neotropical Region, Part VI. Riodinidae*. Hill House, Victoria, Australia.
- Alexander, B. (1990) A cladistic analysis of the nomadiine bees (Hymenoptera: Apoidea). *Systematic Entomology*, **15**, 121–152.
- Bates, H.W. (1859) Notes on South American butterflies. *Transactions of the Entomological Society of London*, (2)5(1), 1–11.
- Bates, H.W. (1868) A catalogue of Erycinidae, a family of diurnal Lepidoptera. *Journal of the Linnean Society (London) (Zoology)*, **9**, 373–459.
- Beutelspacher, C.R. (1981) Una nueva especie mexicana del género *Theope* Doubleday, 1858 [sic] (Lepidoptera: Riodinidae). *Anales del Instituto Biología Universidad Nacional Autónoma México (Zoology)*, **50**, 485–489.
- Bremer, K. (1988) The limits of amino acid sequence data in angiosperm phylogenetic reconstruction. *Evolution*, **42**, 795–803.
- Bremer, K. (1994) Branch support and tree stability. *Cladistics*, **1**, 295–304.
- Brévignon, C. & Gallard, J.-Y. (1995) Contributions à l'étude de Riodinidae des Guyane Française (Lepidoptera). Le genre *Argyrogrammana* Strand, 1932. *Lambillionea*, **95**, 393–406.
- Brévignon, C. & Gallard, J.-Y. (1997a) Inventaire des Riodinidae de Guyane Française. I. Euselasiinae (= Nemeobiinae). Description de nouvelles sous-espèces. (Lepidoptera: Riodinidae). *Lambillionea*, **97**, 264–276.
- Brévignon, C. & Gallard, J.-Y. (1997b) Inventaire des Riodinidae de Guyane Française. II-Riodininae: Mesosemiini, Eurybiini, *incertae sedis*. Description de nouveaux taxa. (Lepidoptera). *Lambillionea*, **97**, 322–342.
- Brévignon, C. & Gallard, J.-Y. (1998a) Inventaire des Riodinidae de Guyane Française. IV-Riodininae: Symmachiini, Charitini, Helicopini. Description de nouveaux taxa. *Lambillionea*, **98**, 304–320.
- Brévignon, C. & Gallard, J.-Y. (1998b) Inventaire des Riodinidae de Guyane Française. III. Riodininae: Riodinini. Description de nouveaux taxa. (Lepidoptera). *Lambillionea*, **98**, 7–24.
- Brévignon, C. & Gallard, J.-Y. (1998c) Inventaire des Riodinidae de Guyane Française. V-Riodininae: 'Emesini', Lemoniini. Description de nouveaux taxa. (Lepidoptera). *Lambillionea*, **98**, 483–498.
- Bridges, C.A. (1994) *Catalogue of the Family-Group, Genus-Group and Species-Group Names of the Riodinidae and Lycaenidae (Lepidoptera) of the World*. C. Bridges, Urbana, Illinois.
- Brower, A.V.Z. (1994) Parallel race formation and the evolution of mimicry in *Heliconius* butterflies: a phylogenetic hypothesis from mitochondrial DNA sequences. *Evolution*, **50**, 195–221.
- Brown, K.S. & Freitas, A.V.L. (1994) Juvenile stages of Ithomiinae: overview and systematics (Lepidoptera: Nymphalidae). *Tropical Lepidoptera*, **5**, 9–20.
- Callaghan, C.J. (1983) A study of isolating mechanisms among Neotropical butterflies of the subfamily Riodininae. *Journal of Research on the Lepidoptera*, **21**, 159–176.
- Callaghan, C.J. (1997) A review of the genus *Panara* Doubleday, 1847 (Riodinidae) in southeast Brazil, with a description of two new subspecies. *Journal of Research on the Lepidoptera*, **34**, 21–38.
- Campbell, D. (1998) *Higher-Level Phylogeny and Molecular Evolution of the Riodinidae (Lepidoptera)*. PhD Dissertation, Harvard University, Cambridge.
- Campbell, D., Brower, A.V.Z. & Pierce, N.E. (2000) Molecular evolution of the *wingless* gene and its implications for the phylogenetic placement of the butterfly family Riodinidae (Lepidoptera: Papilionoidea). *Molecular Biology and Evolution*, **17**, 684–696.
- Carpenter, J.M. (1988) Choosing among multiple equally parsimonious cladograms. *Cladistics*, **4**, 173–179.
- Comstock, J.H. & Needham, J.G. (1918) The wings of insects. *American Naturalist*, **32**, 231–257.
- DeVries, P.J. (1988) The larval ant-organs of *Thisbe irenea* (Lepidoptera: Riodinidae) and their effects upon attending ants. *Zoological Journal of the Linnean Society*, **94**, 379–393.
- DeVries, P.J. (1990) Enhancement of symbioses between butterfly caterpillars and ants by vibrational communication. *Science*, **248**, 1104–1106.
- DeVries, P.J. (1991a) Ecological and evolutionary patterns in riodinid butterflies. *Interactions Between Ants and Plants* (ed. by

- C. Huxley and D. F. Cutler), pp. 143–157. Oxford University Press, Oxford.
- DeVries, P.J. (1991b) Call production by myrmecophilous riordinid and lycaenid butterfly caterpillars (Lepidoptera): morphological, acoustical, functional and evolutionary patterns. *American Museum Novitates*, **3025**, 1–23.
- DeVries, P.J. (1991c) The mutualism between *Thisbe irenea* and ants, and the role of ant ecology in the evolution of larval–ant associations. *Biological Journal of the Linnean Society*, **43**, 179–195.
- DeVries, P.J. (1997) *The Butterflies of Costa Rica and Their Natural History II: Riodinidae*. Princeton University Press, Princeton, New Jersey.
- DeVries, P.J., Chacón, I.A. & Murray, D. (1994) Toward a better understanding of host use and biodiversity in riordinid butterflies (Lepidoptera). *Journal of Research on the Lepidoptera*, **31**, 103–126.
- DeVries, P.J. & Hall, J.P.W. (1996) Two new species of Costa Rican butterflies (Lepidoptera: Riodinidae). *Tropical Lepidoptera*, **7**, 87–90.
- DeVries, P.J., Kitching, I.J. & Vane-Wright, R.I. (1985) The systematic position of *Antirrhea* and *Caerois*, with comments on the classification of the Nymphalidae (Lepidoptera). *Systematic Entomology*, **10**, 11–32.
- DeVries, P.J. & Poinar, G.O. (1997) Ancient butterfly–ant symbiosis: direct evidence from Dominican amber. *Proceedings of the Royal Society of London B*, **264**, 1137–1140.
- Downey, J.C. & Allyn, A.C. (1975) Wing-scale morphology and nomenclature. *Bulletin of the Allyn Museum*, **31**, 1–32.
- Eliot, J.N. (1973) The higher classification of the Lycaenidae (Lepidoptera): a tentative arrangement. *Bulletin of the British Museum of Natural History (Entomology)*, **28**, 373–506.
- Eriksson, T. (1998) *AUTODECAY, Version 4.0*. Department of Botany, Stockholm University, Stockholm, distributed by the author.
- Farris, J.S. (1969) A successive approximations approach to character weighting. *Systematic Zoology*, **18**, 374–385.
- Felsenstein, J.F. (1985) Confidence limits on phylogenies: an approach using the bootstrap. *Evolution*, **39**, 783–791.
- Forbes, W.T.M. (1957) The lycaenid antennae. *Lepidopterists' News*, **11**, 13–14.
- Godman, F.D. & Salvin, O. (1879–1901) *Biologia Centrali-Americana. Insecta. Lepidoptera Rhopalocera*. Dulau & Co, Bernard Quaritch, London.
- Graybeal, A. (1998) Is it better to add taxa or characters to a difficult phylogenetic problem. *Systematic Biology*, **47**, 9–17.
- Guppy, P.J.L. (1904) Notes on the habits and early stages of some Trinidad butterflies. *Transactions of the Entomological Society of London*, **1904**, 225–228.
- Hall, J.P.W. (1998a) Six new species in the 'foliorum group' of *Theope* (Lepidoptera: Riodinidae). *Lambillionea*, **98**, 562–573.
- Hall, J.P.W. (1998b) A review of the genus *Sarota* (Lepidoptera: Riodinidae). *Tropical Lepidoptera*, **9** (Suppl. 1), 1–21.
- Hall, J.P.W. (1999a) *A Revision of the Genus Theope: its Systematics and Biology (Lepidoptera: Riodinidae: Nymphidiini)*. Scientific Publishers, Gainesville, Florida.
- Hall, J.P.W. (1999b) *The Genus Theope and Relatives: Their Systematics and Biology (Lepidoptera: Riodinidae: Nymphidiini)*. PhD Dissertation, University of Florida, Gainesville, Florida.
- Hall, J.P.W. (2000) Two new genera in the Neotropical riordinid tribe Nymphidiini (Riodinidae). *Journal of the Lepidopterists' Society*, **54**, 41–46.
- Hall, J.P.W. & Harvey, D.J. (1998) A new genus of riordinid, with a new species from Panama (Lepidoptera: Riodinidae: Nymphidiini). *Tropical Lepidoptera*, **9** (Suppl. 1), 36–40.
- Hall, J.P.W. & Harvey, D.J. (2001) A reassessment of *Calociasma* with the description of a new genus and a new species (Lepidoptera: Riodinidae: Nymphidiini). *Journal of the New York Entomological Society*, **10**, 196–205.
- Hall, J.P.W. & Heppner, J.B. (1999) Lemoniadini, a corrected tribal name in the Riodininae (Lepidoptera: Riodinidae). *Tropical Lepidoptera*, **10**, 30.
- Hall, J.P.W. & Willmott, K.R. (1995a) Notes on the genus *Argyrogrammana*, with descriptions of five new species (Lepidoptera: Riodinidae). *Tropical Lepidoptera*, **6**, 136–143.
- Hall, J.P.W. & Willmott, K.R. (1995b) Five new species and a new genus of riordinid from the cloud forests of eastern Ecuador (Lepidoptera: Riodinidae). *Tropical Lepidoptera*, **6**, 131–135.
- Hall, J.P.W. & Willmott, K.R. (1996a) Notes on the genus *Argyrogrammana*, part 2, with one new species (Lepidoptera: Riodinidae). *Tropical Lepidoptera*, **7**, 71–80.
- Hall, J.P.W. & Willmott, K.R. (1996b) Systematics of the riordinid tribe Symmachiini, with the description of a new genus and five new species from Ecuador, Venezuela and Brazil (Lepidoptera: Riodinidae). *Lambillionea*, **96**, 637–658.
- Hall, J.P.W. & Willmott, K.R. (1998a) Three new species of Riodinini from the cloud forests of Ecuador (Lepidoptera: Riodinidae). *Tropical Lepidoptera*, **9** (Suppl. 1), 22–26.
- Hall, J.P.W. & Willmott, K.R. (1998b) Nine new species and one new subspecies of *Euselasia* from Ecuador (Lepidoptera: Riodinidae). *Tropical Lepidoptera*, **9** (Suppl. 1), 27–35.
- Harvey, D.J. (1987) *The Higher Classification of the Riodinidae (Lepidoptera)*. PhD Dissertation, University of Texas, Austin, Texas.
- Hendy, M.D. & Penny, D. (1989) A framework for the quantitative study of evolutionary trees. *Systematic Zoology*, **38**, 297–309.
- Heppner, J.B. (1991) Faunal regions and the diversity of Lepidoptera. *Tropical Lepidoptera*, **2** (Suppl. 1), 1–85.
- Heppner, J.B. (1998) Classification of Lepidoptera. Part 1. Introduction. *Holarctic Lepidoptera*, **5** (Suppl. 1), 1–148.
- Herrich-Schäffer, G.A.W. (1843–1856) *Systematische Bearbeitung der Schmetterlinge von Europa, Zeugleich als Text, Revision und Supplement zu J. Hübner's Sammlung Europäischer Schmetterlinge*. 6 Volumes. G. Manz, Regensburg.
- Hillis, D.M. (1996) Inferring complex phylogenies. *Nature*, **383**, 130.
- Hillis, D.M. (1998) Taxonomic sampling, phylogenetic accuracy, and investigator bias. *Systematic Biology*, **47**, 3–8.
- Iturralde-Vinent, M.A. & MacPhee, R.D.E. (1996) Age and paleogeographic origin of Dominican amber. *Science*, **273**, 1850–1852.
- Kitching, I.J. (1985) Early stages and the classification of milkweed butterflies (Lepidoptera: Danainae). *Zoological Journal of the Linnean Society*, **85**, 1–97.
- Klots, A.B. (1956) Lepidoptera. *Taxonomists's Glossary of Genitalia in Insects* (ed. by S. L. Tuxen), pp. 97–110. Munksgaard, Copenhagen.
- Lecointre, G., Philippe, H., Lanh Van Lê, H. & Le Guyader, H. (1993) Species sampling has a major impact on phylogenetic inference. *Molecular Phylogenetics and Evolution*, **2**, 205–224.
- Liebherr, J.K. & Zimmerman, E.C. (1998) Cladistic analysis, phylogeny and biogeography of the Hawaiian Platynini (Coleoptera: Carabidae). *Systematic Entomology*, **23**, 137–172.
- Maddison, D.R. (1991) The discovery and importance of multiple islands of most parsimonious trees. *Systematic Zoology*, **40**, 315–328.
- Maddison, W.P. & Maddison, D.R. (1995) *MacClade: Analysis of Phylogeny and Character Evolution, Version 3.05*. Sinauer Associates, Sunderland, Massachusetts.

- Miller, J.S. (1988) External genitalic morphology and copulatory mechanism of *Cyanotricha necyria* (Felder) (Noctuoidea: Dioptriidae). *Journal of the Lepidopterists' Society*, **42**, 103–115.
- Miller, J.S. (1991) Cladistics and classification of the Notodontidae (Lepidoptera: Noctuoidea) based on larval and adult morphology. *Bulletin of the American Museum of Natural History*, **204**, 1–230.
- Miller, J.S. (1996) Phylogeny of the Neotropical moth tribe Josiini (Notodontidae: Dioptriidae): a hidden case of Müllerian mimicry. *Zoological Journal of the Linnean Society*, **118**, 1–45.
- Miller, J.S., Brower, A.V.Z. & DeSalle, R. (1997) Phylogeny of the Neotropical moth tribe Josiini (Notodontidae: Dioptriidae): comparing and combining evidence from DNA sequences and morphology. *Biological Journal of the Linnean Society*, **60**, 297–316.
- Naylor, G.J. (1992) The phylogenetic relationships among requiem and hammerhead sharks: inferring phylogeny when thousands of equally most parsimonious trees result. *Cladistics*, **8**, 295–318.
- Nijhout, H.F. (1991) *The Development and Evolution of Butterfly Wing Patterns*. Smithsonian Institution Press, Washington, DC.
- Parsons, M.J. (1996) Gondwanan evolution of the troidine swallowtails (Lepidoptera: Papilionidae): cladistic reappraisals using mainly immature stage characters, with focus on the birdwings *Ornithoptera* Boisduval. *Bulletin of the Kitakyushu Museum of Natural History*, **15**, 43–118.
- Penz, C.M. (1999) Higher level phylogeny for the passion-vine butterflies (Nymphalidae, Heliconiinae) based on early stage and adult morphology. *Zoological Journal of the Linnean Society*, **127**, 277–344.
- Penz, C.M. & DeVries, P.J. (1999) Preliminary assessment of the tribe Lemoniini (Lepidoptera: Riodinidae) based on adult morphology. *American Museum Novitates*, **3284**, 1–32.
- Robbins, R.K. (1982) How many butterfly species? *News of the Lepidopterists' Society*, **1982**, 40–41.
- Robbins, R.K. (1991) Evolution, comparative morphology, and identification of the eumaeine butterfly genus *Rekoa* Kaye (Lycaenidae: Theclinae). *Smithsonian Contributions to Zoology*, **498**, 1–64.
- Robbins, R.K. (1993) Comparison of butterfly diversity in the Neotropical and Oriental regions. *Journal of the Lepidopterists' Society*, **46**, 298–300.
- Robbins, R.K., Lamas, G., Mielke, O.H.H., Harvey, D.J. & Casagrande, M.M. (1996) Taxonomic composition and ecological structure of the species-rich butterfly community at Pakitza, Parque Nacional del Manu, Perú. *Manu: the Biodiversity of Southeastern Peru* (ed. by D. E. Wilson and A. Sandoval), pp. 217–252. Smithsonian Institution Press, Washington, DC.
- Sanderson, M.J. (1995) Objections to bootstrapping phylogenies: a critique. *Systematic Biology*, **44**, 299–320.
- Sanderson, M.J. & Donoghue, M.J. (1989) Patterns of variation in levels of homoplasy. *Evolution*, **43**, 1781–1795.
- Scoble, M.J. (1992) *The Lepidoptera: Form, Function and Diversity*. Oxford University Press, London.
- Seitz, A. (1916–20) Familie Erycinidae. *Die Gross-Schmetterlinge der Erde*, Vol. 5 (ed. by A. Seitz), pp. 617–728. Alfred Kernen, Stuttgart.
- Stichel, H.F.E.J. (1910) Family Riodinidae. Allgemeines. Subfamily Riodininae. *Genera Insectorum*, **112A**, 1–238.
- Stichel, H.F.E.J. (1911) Family Riodinidae. Allgemeines. Subfamily Riodininae. *Genera Insectorum*, **112B**, 239–452.
- Stichel, H.F.E.J. (1928) Lepidoptera Nemeobiinae. *Das Tierreich*, **51**, 1–330.
- Stichel, H.F.E.J. (1930–31) Riodinidae. *Lepidopterorum Catalogus*, Vol. 38–41 (ed. by E. Strand), pp. 1–795. Dr W. Junk, Berlin.
- Swofford, D.L. (1999) *PAUP: Phylogenetic Analysis Using Parsimony (and Other Methods)*, Version 4.0b4a. Sinauer Associates, Sunderland, Massachusetts.
- Vane-Wright, R.I. & Smith, C.R. (1991) Phylogenetic relationships of three African swallowtail butterflies, *Papilio dardanus*, *P. phorcas*, and *P. constantinus*: a cladistic analysis (Lepidoptera: Papilionidae). *Systematic Entomology*, **16**, 275–291.

Accepted 29 January 2001

Appendix 1

Characters employed in the cladistic analysis of Theopeina. Unless otherwise stated, taxa for which a character is inapplicable are coded in two different ways: in cases where the states of a character are based on an apomorphic state from a previous character they are coded with a '0' and where the states of a character are based on a plesiomorphic state from a previous character they are coded with a '?'. The Consistency Index (CI) and Retention Index (RI), based on the cladogram in Figs 4 and 5, and references to figures are given for each character.

Behavioural ecology

1. *Adults rest with wings*: (0) outspread; (1) closed over body. CI = 0.5; RI = 0.67.

Character states are applied largely on the basis of my own field work but in a few instances information has been received from C. Brévignon, M. Cock, P. DeVries, J.-Y. Gallard and R. Robbins (personal communication).

Character state (0) is typical for Riodinidae and state (1) occurs elsewhere in Nymphidiini only in *Setabis*.

Wing shape

2. *Base of forewing costa*: (0) straight or mildly arched (e.g. Fig. 1H); (1) pronouncedly arched (Fig. 1T). CI = 0.5; RI = 0.88.
3. *A serrate distal hindwing margin*: (0) absent; (1) present (Fig. 1D). CI = 1; RI = 1.
4. *A bulbously pronounced anal fold*: (0) absent; (1) present (Fig. 1V). CI = 0.5; RI = 0.67.

Wing pattern

5. *Dorsal surface of male*: (0) blue and/or white (e.g. Fig. 1J); (1) patterned orange (Fig. 1B); (2) uniform orange (Fig. 1M); (3) entirely brown (e.g. Fig. 1H). CI = 0.75; RI = 0.83.

6. *A white triangle at middle of dorsal forewing costa*: (0) absent; (1) present (Fig. 1E). CI = 1; RI = 1.
7. *Contrasted area of postdiscal pale brown scales on dorsal forewing of males*: (0) absent; (1) present (e.g. Fig. 1N). CI = 0.25; RI = 0.7.
See Hall (1999a) for an SEM illustration of character state (1).
8. *Costal area of contrasted pale brown scales on dorsal hindwing of males*: (0) absent; (1) present (Fig. 1T). CI = 0.5; RI = 0.8.
See Hall (1999a) for an SEM illustration of character state (1).
9. *An isolated subapical blue patch on dorsal forewing of females*: (0) absent (e.g. Fig. 1K); (1) present (Fig. 1Q). CI = 0.33; RI = 0.67.
10. *An elongate postdiscal blue extension in cells M2 and M1 only on dorsal forewing of females*: (0) absent (e.g. Fig. 1W); (1) present (Fig. 1U). CI = 1; RI = 1.
11. *An elongate postdiscal blue extension that includes cell M3 on dorsal forewing of females*: (0) absent (e.g. Fig. 1W); (1) present (Fig. 1L). CI = 0.33; RI = 0.33.
12. *Ventral ground colour of male*: (0) predominantly various shades of white, cream or brown (e.g. Fig. 2H); (1) entirely shades of yellow (e.g. Fig. 2N). CI = 0.33; RI = 0.88.
13. *If ventral ground colour of male a shade of yellow (12:1)*: (1) matte yellow (Fig. 2M); (2) chrome yellow (Fig. 2N); (3) orange (Fig. 2K). CI = 0.6; RI = 0.86.
14. *Contrasted darker scaling at distal margins of both ventral wing surfaces*: (0) absent; (1) present (Fig. 2K). CI = 1; RI = 1.
15. *Blue or purple iridescence on ventral surface*: (0) absent; (1) present (Fig. 2V). CI = 1; RI = 1.
16. *Prominent yellow scaling at base only of ventral forewing*: (0) absent; (1) present (Fig. 2V). CI = 1; RI = 1.
17. *If prominent yellow scaling at base of ventral forewing only present (16:1)*: (1) of same extent in both sexes; (2) of greater extent in females (Fig. 2V,W). CI = 1; RI = 1.
18. *Red scaling at base of ventral forewing*: (0) absent; (1) present (Fig. 2J). CI = 1; RI = 1.
19. *Fine scaled yellow banding ('ripple pattern') on ventral surface*: (0) absent; (1) present (Fig. 2G). CI = 1; RI = 1.
20. *Two spots at base of cell Cu₂ on ventral forewing*: (0) present (e.g. Fig. 2C); (1) absent (e.g. Fig. 2H). CI = 1; RI = 1.
21. *White spot in middle of discal cell of ventral forewing*: (0) absent; (1) present (Fig. 2R). CI = 1; RI = 1.
22. *A postdiscal line of disjointed spots on ventral forewing*: (0) absent; (1) present (Fig. 2C). CI = 0.5; RI = 0.67.
23. *A medial white band on both ventral wing surfaces*: (0) absent; (1) present (Fig. 2O). CI = 1; RI = 1.
24. *A single dark brown transverse band on ventral forewing*: (0) absent; (1) present (e.g. Fig. 2R). CI = 1; RI = 1.
25. *If a single dark brown transverse band on ventral forewing present (24:1), it originates from*: (1) approximately mid-point of costa (Fig. 2S); (2) near apex (Fig. 2R). CI = 1; RI = 1.

26. *Thin, contrasted yellow line at distal margin of both ventral wing surfaces*: (0) absent; (1) present (e.g. Fig. 2H). CI = 1; RI = 1.
27. *Black submarginal spots on ventral surface*: (0) present (e.g. Fig. 2H); (1) absent (e.g. Fig. 2N). CI = 0.13; RI = 0.75.

Character state (0) is applied to a taxon if either sex or any population exhibit such spots.

28. *If ventral submarginal spots present (27:0), spots*: (0) evenly distributed on forewing (e.g. Fig. 2H); (1) restricted to apex on forewing (Fig. 2G). CI = 0.5; RI = 0.67.
29. *If ventral submarginal spots present (27:0), spots*: (0) approximately of even size on hindwing (e.g. Fig. 2H); (1) enlarged in apex of hindwing (Fig. 2G). CI = 1; RI = 1.
30. *If ventral submarginal spots present (27:0), spots*: (0) surrounded by white scaling or no additional scaling (e.g. Fig. 2H); (1) bluish-white scaling (e.g. Fig. 2R). CI = 1; RI = 1.

Male abdomen

31. *Blue scaling over entire dorsal surface of abdomen*: (0) absent (e.g. Fig. 1U); (1) present (e.g. Fig. 1R). CI = 0.5; RI = 0.91.
32. *An isolated patch of smaller, paler coloured scales on dorsum of male abdomen*: (0) absent; (1) brown and restricted to segment 3 (Fig. 1M); (2) whitish and present on segments 2 and 3 (Fig. 1U). CI = 0.67; RI = 0.75.
See Hall (1999a) for illustrations of character states (1) and (2).
33. *A thin, contrasted whitish line along length of ventral abdominal surface*: (0) absent (e.g. Fig. 2U); (1) present (Fig. 2J). CI = 1; RI = 0.
34. *Spiracle on abdominal segment 3 of males positioned*: (0) dorsally (Fig. 6A); (1) medially (Fig. 6B); (2) ventrally (Fig. 6C). CI = 1; RI = 0.

As the only male abdomen available for *A. drepana* was damaged and no male is known for *A. urichi*, this character was coded from the female abdomen for these two species.

35. *Eighth male tergite*: (0) a continuously even ventral margin (e.g. Fig. 6H); (1) a sharply indented ventral margin medially (Fig. 6D); (2) a sharply indented ventral margin anteriorly (Fig. 6E). CI = 0.5; RI = 0.5.
36. *A small, ovoid, lightly sclerotized fenestration in middle of eighth male tergite*: (0) absent; (1) present (Fig. 6I). CI = 1; RI = 1.
37. *Eighth male tergite*: (0) symmetrical; (1) asymmetrical (Fig. 6J). CI = 0.33; RI = 0.6.
38. *Eighth male tergite*: (0) roughly square (length < 6 × width) (e.g. Fig. 6E); (1) elongate (length > 6 × width) (Fig. 6F). CI = 0.25; RI = 0.25.

Length is measured from anterior tip to posterior tip; height is measured at a point towards posterior tip.

39. *A sclerotized invagination at posterior margin of eighth male tergite*: (0) absent; (1) present on at least one side of abdomen (e.g. Fig. 6H). CI = 0.2; RI = 0.86.
40. *If a sclerotized invagination present at posterior margin of eighth male tergite (39:1), invagination*: (1) narrow on both sides of abdomen (Fig. 6H); (2) broad on at least one side of abdomen (Fig. 6J). CI = 0.25; RI = 0.78.
41. *A projection from posterior margin of eighth male tergite*: (0) absent; (1) typically small, blunt (Fig. 6D); (2) bifurcate (Fig. 6G); (3) typically long, 'spike'-like (e.g. Fig. 6H). CI = 0.25; RI = 0.76.

Character state (2) is derived from an illustration in Beutelspacher (1981).

42. *Anterior margin of eighth male tergite*: (0) straight or smoothly rounded (e.g. Fig. 6H); (1) pronouncedly angular (e.g. Fig. 6J). CI = 0.17; RI = 0.78.
43. *A dorsal sclerotized invagination on eighth male sternite*: (0) absent; (1) present (e.g. Fig. 7B). CI = 1; RI = 1.
44. *If a dorsal sclerotized invagination present on eighth male sternite (43:1), invagination*: (1) restricted to posterior half of sternite (Fig. 7B); (2) connected to genital armature (e.g. Fig. 8A). CI = 1; RI = 1.
45. *Ventral portion of eighth male sternite*: (0) entire (e.g. Fig. 7I); (1) reduced to a tiny vestigial triangle or band (e.g. Fig. 7K). CI = 0.5; RI = 0.97.
46. *Ventral portion of eighth male sternite*: (0) symmetrical; (1) asymmetrical (Fig. 7B). CI = 1; RI = 1.
47. *Dorsal portion of eighth male sternite*: (0) symmetrical; (1) asymmetrical (e.g. Fig. 7K). CI = 1; RI = 1.
48. *Lateral projections from eighth male sternite*: (0) absent; (1) present (e.g. Fig. 7G). CI = 0.5; RI = 0.96.
49. *If lateral projections from eighth male sternite: present (48:1), projections*: (1) very small (Fig. 7D); (2) small to large (e.g. Fig. 7I). CI = 0.67; RI = 0.96.
50. *Eighth male sternite*: (0) a plain rectangle (Fig. 7A); (1) large with 2 posteriorly pointing projections (Fig. 7B); (2) small, long, narrow and ribbonlike (Fig. 7C); (3) long and of medium width with a small posterior projection and tiny lateral flanges (Fig. 7D); (4) broad with a variably sized posterior projection and small to medium lateral flanges (Fig. 7E); (5) narrowly pointed with small lateral flanges (Fig. 7F); (6) large and laterally compressed, thus narrow in ventral view but broad in lateral view (Fig. 7G); (7) formed into a narrow, posteriorly projecting 'horn' (Fig. 7J); (8) broad with a medium to large posterior projection and 2 very long dorsoposterior projections (Fig. 7I); (9) formed into 2 angular dorsoposterior projections (Fig. 7H); (A) reduced to a vestigial triangle ventrally but dorsal invagination is produced into a very long dorsoposterior left projection and a shorter right projection (Fig. 7K); (B) reduced to a vestigial triangle ventrally but dorsal invagination is produced into 2 very long dorsoposterior projections that are bifurcate towards their tip (Fig. 7L); (C) reduced to a vestigial triangle (Fig. 7D); (D) reduced to a vestigial band (Fig. 7B). CI = 0.93; RI = 0.98.

Male genitalia

51. *A lightly sclerotized region at posterior margin of uncus*: (0) absent; (1) present (e.g. Fig. 8B). CI = 0.5; RI = 0.
52. *If a lightly sclerotized region at posterior margin of uncus present (51:1), region*: (1) does not extend to leave a heavily sclerotized triangle at lower corner (e.g. Fig. 8B); (2) does extend to leave a heavily sclerotized triangle at lower corner (Fig. 8D). CI = 0.67; RI = 0.80.
53. *A small anterior region devoid of setae on dorsal portion of uncus*: (0) absent; (1) present (Fig. 8C). CI = 0.25; RI = 0.75.
54. *Setae on uncus*: (0) evenly distributed; (1) largely restricted to dorsal half (e.g. Fig. 8A). CI = 0.25; RI = 0.5.
55. *A large, upper posterior extension to uncus differentiated from lower portion*: (0) absent (e.g. Fig. 9D); (1) present (e.g. Fig. 9G). CI = 1; RI = 1.
56. *Upper portion of uncus*: (0) rounded (e.g. Fig. 9F); (1) downwardly pointed (e.g. Fig. 9G). CI = 1; RI = 1.
57. *Lower portion of uncus*: (0) undifferentiated from upper portion or evenly triangular (e.g. Fig. 9B); (1) triangular and downwardly pointed (Fig. 9E); (2) a narrowly elongate triangle (Fig. 9F); (3) a broadly elongate triangle (Fig. 9A); (4) produced into one or 2 small points (e.g. Fig. 9C). CI = 0.8; RI = 0.96.
58. *Tegumen*: (0) an approximate triangle (e.g. Fig. 9C); (1) a narrow rectangle (Fig. 9B); (2) very elongate, especially in lower anterior corner (Fig. 9E). CI = 0.67; RI = 0.75.
59. *Falces*: (0) of average length and width (e.g. Fig. 9C); (1) very long and thin (Fig. 9H); (2) compact and squarely angular (Fig. 9D); (3) bulbously rounded (Fig. 9B); (4) rectangular at base ($> 90^\circ$), lower edge convex, remainder long and upwardly pointed (e.g. Fig. 9F); (5) dorso-ventrally compressed (Fig. 9I); (6) rectangular at base ($< 90^\circ$), lower edge straight or concave, remainder short, straight and pointed (e.g. Fig. 9G); (7) rectangular at base ($< 90^\circ$), lower edge convex, remainder long and rounded, often with tip turned outwards (Fig. 9E). CI = 1; RI = 1.
60. *Vinculum extends from anterior edge of tegumen to*: (0) beyond top of valvae (e.g. Fig. 8B); (1) top of valvae (Fig. 8D). CI = 1; RI = 1.
61. *A posterior projection from medial region of vinculum*: (0) absent; (1) present (e.g. Fig. 9K). CI = 1; RI = 1.
62. *If a posterior projection from medial region of vinculum is present (61:1), projection*: (1) a small 'hump' (Fig. 9K); (2) an elongate triangle (Fig. 9L). CI = 1; RI = 1.
63. *A posterior projection from upper region of vinculum*: (0) absent; (1) present (e.g. Fig. 9M). CI = 1; RI = 1.
64. *If a posterior projection from upper region of vinculum is present (63:1), projection*: (1) long and triangular on both sides (Fig. 9M); (2) very long and 'paddle'-shaped on at least one side (Fig. 9N). CI = 0.67; RI = 0.8.
65. *Vinculum*: (0) symmetrical; (1) asymmetrical (Fig. 9N). CI = 0.5; RI = 0.67.

66. *Vinculum forms*: (0) a true anterior saccus (Fig. 9J); (1) a ventral, anterior 'bulb' (Fig. 9A); (2) a ventral, posterior 'cup' (Fig. 8B); (3) no anterior or posterior shapes ventrally (e.g. Fig. 9N). CI = 0.75; RI = 0.9.
67. *Valvae*: (0) narrow, elongate and pointed (Fig. 10A); (1) very large and broad with 2 rounded projections (Fig. 10D); (2) large and broad with single, 'bird's-head'-shaped upper projection (Fig. 10C); (3) broad with narrow, upwardly pointed upper projection and rounded lower projection (Fig. 10B); (4) small with upwardly pointed upper projection and smaller lower projection (Fig. 10G); (5) narrow with prominent basal lateral bulge and narrow upwardly pointed projection (Fig. 10H); (6) small and narrow with one or 2 rounded points at tip (Fig. 10F); (7) large, posteriorly elongate and rounded at tip (Fig. 10I); (8) square or rectangular with concave distal margin (Fig. 10J); (9) roundly rectangular with single posteriorly projecting point at middle of distal margin (Fig. 10K); (A) dorsally elongate and narrow with short basal lateral bulge (Fig. 10N); (B) large and dorsally very elongate with posteriorly projecting semicircle at dorsal tip (e.g. Fig. 10M); (C) variably elongate with distal undulations and concave anterior margin towards tip (Fig. 10L); (D) large and markedly bifurcate with very long and narrow lower projection and large basal lateral bulge (Fig. 10E); (E) dorsally elongate and narrow, twisted toward rounded tip (e.g. Fig. 10S); (F) large and bifurcate with prominent basal lateral bulge and narrow posterior projection at middle of distal margin that broadens at tip (Fig. 10R); (G) large, narrow and dorsally elongate with equally broad anterior margin (Fig. 10O); (H) large with variably elongate, narrow upper posterior projection (an upper 'arm') (e.g. Fig. 10U); (I) triangular and dorsally elongate, tilted inwards dorsally over aedeagus with tips splayed outwards (Fig. 10Q); (J) narrow with basal lateral bulge of same length as remainder (Fig. 10P). CI = 1; RI = 1.
68. *If upper 'arms' to valvae present (67:H), 'arms'*: (1) small (Fig. 10T); (2) long (Fig. 10U); (3) very long (Fig. 10V). CI = 1; RI = 1.
69. *If upper 'arms' to valvae present (67:H), a basal 'hump'*: (1) absent; (2) present (Fig. 10V). CI = 1; RI = 1.
70. *If upper 'arms' to valvae present (67:H), in dorsal view 'arms'*: (1) lie close together at base (e.g. Fig. 10U); (2) are distantly separated at base (Fig. 10V). CI = 1; RI = 1.
71. *Posterior portion of aedeagus*: (0) straight or downturned (e.g. Fig. 11E); (1) up-turned (e.g. Fig. 11H). CI = 0.33; RI = 0.93.
72. *Tip of aedeagus*: (0) variably pointed or rounded (e.g. Fig. 11B); (1) abruptly up-turned and vertically broad (Fig. 11G); (2) bulbous and 'basket'-shaped (e.g. Fig. 11I). CI = 1; RI = 1.
73. *If tip of aedeagus is bulbous and 'basket'-shaped (72:2), tip*: (1) small, well sclerotized and highly torsional (Fig. 11I); (2) large and semi-sclerotized (Fig. 8D). CI = 1; RI = 1.
74. *Lightly sclerotized lateral tissue towards tip of aedeagus*: (0) absent; (1) present (Fig. 11D). CI = 1; RI = 1.
75. *Aedeagal tip opens*: (0) upwards, posteriorly or weakly to the left (e.g. Fig. 11F); (1) markedly to the right (Fig. 11C). CI = 0.5; RI = 0.67.
76. *Aedeagus*: (0) straight towards anterior end (e.g. Fig. 11E); (1) contorted towards anterior end (e.g. Fig. 11I). CI = 0.33; RI = 0.9.
77. *Soft tissue at anterior tip of aedeagus*: (0) directed anteriorly (e.g. Fig. 11G); (1) ventrally (Fig. 11C). CI = 1; RI = 1.
78. *A sclerotized plate inside aedeagus*: (0) absent; (1) present (Fig. 11G). CI = 1; RI = 1.
- This character is coded separately from the following as it varies independently.
79. *Aedeagus contains*: (0) several sparsely distributed, variably elongate and heavily sclerotized pencillate cornuti (Fig. 11B); (1) a long band of numerous small, triangular and oval cornuti (Fig. 11C); (2) numerous, densely packed long pencillate cornuti (Fig. 8A); (3) a single large crescent-shaped cornutus (Fig. 11A); (4) a single, elongate and narrow cornutus that parallels distal edge of aedeagus when everted (Fig. 11D); (5) one or more triangular cornuti that are heavily sclerotized only at tip and project anteriorly when everted (e.g. Fig. 11E); (6) a single, large, arrow-shaped cornutus (Fig. 11G); (7) one or typically more, medium sized, triangular or teardrop shaped cornuti (Fig. 8D); (8) no internal cornuti or only tiny sclerotized structures (e.g. Fig. 11H). CI = 1; RI = 1.
80. *If one or more triangular cornuti that are heavily sclerotized only at tip are present (79:5), cornuti*: (1) solitary (Fig. 11E); (2) paired (Fig. 11F). CI = 1; RI = 1.
81. *Pediceal*: (0) normal and straplike (Fig. 8B); (1) is laterally thickened (Fig. 8A); (2) consists of a well sclerotized base with lightly sclerotized remainder (Fig. 8D). CI = 0.67; RI = 0.92.
82. *Pediceal*: (0) symmetrical; (1) asymmetrical (e.g. Fig. 11J). CI = 1; RI = 1.
83. *If pedicel asymmetrical (82:1), asymmetry*: (1) weak (Fig. 11J); (2) very pronounced (Fig. 11K). CI = 1; RI = 1.

Female abdomen and genitalia

84. *A heavily sclerotized disc at upper posterior margin of last tergite*: (0) absent; (1) present (e.g. Fig. 13B). CI = 0.25; RI = 0.84.
85. *If a heavily sclerotized disc at upper posterior margin of last tergite present (84:1), disc*: (1) small and semi-circular (Fig. 13A); (2) posteriorly elongate (Fig. 13B). CI = 0.33; RI = 0.8.
86. *A variably sclerotized plate with a pair of indentations between ostium bursae and papillae anales*: (0) absent; (1) present (Fig. 13F). CI = 0.5; RI = 0.67.
87. *Ostium bursae*: (0) consists of a sclerotized ring (e.g. Fig. 12B); (1) has no entire sclerotized dorsal

portion but only a tiny sclerotized triangle at each dorsal corner (Fig. 13G); (2) has no sclerotized dorsal portion (e.g. Fig. 13E); (3) has no sclerotized ventral portion (Fig. 13H). CI = 0.43; RI = 0.73.

88. *If ostium bursae consists of a sclerotized ring (87:0), ostium:* (0) variably round (e.g. Fig. 12B); (1) elongate and shaped like an 'open mouth' (Fig. 12A). CI = 1; RI = 1.
 89. *If ostium bursae consists of a sclerotized ring (87:0), an elongate dorsolateral projection on either side:* (0) absent; (1) present (Fig. 12D). CI = 1; RI = 1.
 90. *Ventral portion of ostium bursae:* (0) straight or evenly rounded (Fig. 13I); (1) formed into an angular 'U'-shape with the tips as broad as or broader than the base (Fig. 13E). CI = 1; RI = 1.
- The single taxon which has no ventral portion to the ostium bursae, *P. senta*, is coded with character state (?).
91. *A triangular, posteriorly concave, anterolateral projection on either side of ostium bursae:* (0) absent; (1) present (Fig. 13J). CI = 1; RI = 1.
 92. *Significant amounts of heavy sclerotization in posterior half of ductus bursae:* (0) absent (e.g. Fig. 12B); (1) present and shorter in length than corpus bursae (e.g. Fig. 12D); (2) present and equal in length to corpus bursae (Fig. 12A). CI = 0.33; RI = 0.71.
 93. *Posterior half of ductus bursae:* (0) straight (e.g. Fig. 12A); (1) to some degree coiled (Fig. 12C). CI = 0.5; RI = 0.67.
 94. *Posterior half of ductus bursae:* (0) approximately parallel with abdomen (e.g. Fig. 12B); (1) angled dorsally towards papillae anales, creating right angle with remainder of ductus bursae (Fig. 12D). CI = 1; RI = 1.
 95. *A hollow, medially divided, sclerotized ovoid structure in ductus bursae opposite opening to ductus seminalis:* (0) absent; (1) present (e.g. Fig. 13C). CI = 1; RI = 1.
 96. *If a hollow, medially divided, sclerotized ovoid structure in ductus bursae opposite opening to ductus seminalis present (95:1), structure:* (1) short (Fig. 13D); (2) long (Fig. 13C). CI = 1; RI = 1.
 97. *If a hollow, medially divided, sclerotized ovoid structure in ductus bursae opposite opening to ductus seminalis present (95:1), structure positioned:* (1) close to

ostium bursae (Fig. 13C); (2) far from ostium bursae (Fig. 13D). CI = 1; RI = 0.

98. *A small, heavily sclerotized 'bean'-shaped structure in ductus bursae between ductus seminalis and opening to corpus bursae:* (0) absent; (1) present (Fig. 12A). CI = 1; RI = 1.
99. *Ductus seminalis:* (0) a small tube extending at approximate right angle from ductus bursae (e.g. Fig. 12A); (1) a broad tube extending in seamless straight line from middle of ductus bursae; posterior portion of ductus bursae extends from this junction as smaller tube (Fig. 12D). CI = 1; RI = 1.
100. *Ductus seminalis:* (0) not hardened; (1) hardened (but not sclerotized) with studded sculpturing (Fig. 12B). CI = 0.5; RI = 0.83.
101. *Signa:* (0) sclerotized bands (Fig. 12E); (1) sclerotized invaginations (e.g. Fig. 12C); (2) absent. CI = 1; RI = 1.
102. *If signa form sclerotized invaginations (101:1), their openings at wall of corpus bursae:* (1) broadest horizontally (Fig. 14A); (2) vertically (e.g. Fig. 14G). CI = 0.67; RI = 0.67.
103. *If signa form sclerotized invaginations with vertical openings (102:2), signa:* (1) small, approximate semicircles or rectangles (Fig. 14D); (2) small triangles (e.g. Fig. 14E); (3) rounded with concave distal margins (Fig. 14J); (4) symmetrically pointed at posterior and anterior tips (Fig. 14C); (5) small and narrowly pointed (Fig. 14B); (6) rectangular with small pointed tips (Fig. 14K); (7) elongate at base with serrate inner edges and roundly pointed tips (e.g. Fig. 14L); (8) very large and elongate at base with serrate inner edges and broadly pointed tips (Fig. 14G); (9) sharply pointed triangles with concave anterior margins (e.g. Fig. 14I); (A) very large and elongate at base with very long roundly pointed tips (Fig. 14F); (B) very large and elongate at base with very large and broadly rounded tips (e.g. Fig. 14H). CI = 0.79; RI = 0.90.
104. *If invaginated signa are very large and elongate at base with very large and broadly rounded tip (103:B), transverse creases across their surface:* (1) absent (Fig. 12A); (2) present (Fig. 14H). CI = 1; RI = 1.

[illegible]

Appendix 2. Continued.

	5	1	0	1	2	2	3	3	4	4	5	5	5	6	6	7	7	8	8	9	9	0	1
<i>Theope antanitis</i>	?	0	0	0	0	0	0	0	0	0	0	0	0	0	0	0	0	0	0	0	0	0	?
<i>Theope tani</i>	1	0	0	0	0	0	0	0	0	0	0	0	0	0	0	0	0	0	0	0	0	0	?
<i>Theope villai</i>	?	0	0	0	0	0	0	0	0	0	0	0	0	0	0	0	0	0	0	0	0	0	?
<i>Theope virgilius</i>	1	0	0	0	0	0	0	0	0	0	0	0	0	0	0	0	0	0	0	0	0	0	?
<i>Theope eupolis</i>	1	0	0	0	0	0	0	0	0	0	0	0	0	0	0	0	0	0	0	0	0	0	?
<i>Theope nobilis</i>	1	0	0	0	0	0	0	0	0	0	0	0	0	0	0	0	0	0	0	0	0	0	?
<i>Theope publius</i>	1	0	0	0	0	0	0	0	0	0	0	0	0	0	0	0	0	0	0	0	0	0	?
<i>Theope sanjuani</i>	?	0	0	0	0	0	0	0	0	0	0	0	0	0	0	0	0	0	0	0	0	0	?
<i>Theope terambus</i>	1	0	0	0	0	0	0	0	0	0	0	0	0	0	0	0	0	0	0	0	0	0	?
<i>Theope syngenes</i>	1	0	0	0	0	0	0	0	0	0	0	0	0	0	0	0	0	0	0	0	0	0	?
<i>Theope bacenis</i>	1	0	0	0	0	0	0	0	0	0	0	0	0	0	0	0	0	0	0	0	0	0	?
<i>Theope basilea</i>	1	0	0	0	0	0	0	0	0	0	0	0	0	0	0	0	0	0	0	0	0	0	?
<i>Theope comosa</i>	1	0	0	0	0	0	0	0	0	0	0	0	0	0	0	0	0	0	0	0	0	0	?
<i>Theope zostera</i>	1	0	0	0	0	0	0	0	0	0	0	0	0	0	0	0	0	0	0	0	0	0	?
<i>Theope nodosus</i>	1	0	0	0	0	0	0	0	0	0	0	0	0	0	0	0	0	0	0	0	0	0	?
<i>Theope phaeo</i>	1	0	0	0	0	0	0	0	0	0	0	0	0	0	0	0	0	0	0	0	0	0	?
<i>Theope theritis</i>	1	0	0	0	0	0	0	0	0	0	0	0	0	0	0	0	0	0	0	0	0	0	?
<i>Theope thoetes</i>	1	0	0	0	0	0	0	0	0	0	0	0	0	0	0	0	0	0	0	0	0	0	?
<i>Theope apheles</i>	1	0	0	0	0	0	0	0	0	0	0	0	0	0	0	0	0	0	0	0	0	0	?
<i>Theope sobrina</i>	1	0	0	0	0	0	0	0	0	0	0	0	0	0	0	0	0	0	0	0	0	0	?
<i>Theope janus</i>	1	0	0	0	0	0	0	0	0	0	0	0	0	0	0	0	0	0	0	0	0	0	?
<i>Theope guillaumei</i>	1	0	0	0	0	0	0	0	0	0	0	0	0	0	0	0	0	0	0	0	0	0	?
<i>Theope discus</i>	1	0	0	0	0	0	0	0	0	0	0	0	0	0	0	0	0	0	0	0	0	0	?
<i>Theope thestias</i>	1	0	0	0	0	0	0	0	0	0	0	0	0	0	0	0	0	0	0	0	0	0	?
<i>Theope decorata</i>	1	0	0	0	0	0	0	0	0	0	0	0	0	0	0	0	0	0	0	0	0	0	?
<i>Theope lycanina</i>	1	0	0	0	0	0	0	0	0	0	0	0	0	0	0	0	0	0	0	0	0	0	?
<i>Theope leucanth</i>	1	0	0	0	0	0	0	0	0	0	0	0	0	0	0	0	0	0	0	0	0	0	?
<i>Theope amicitiae</i>	1	0	0	0	0	0	0	0	0	0	0	0	0	0	0	0	0	0	0	0	0	0	?
<i>Theope christiani</i>	?	0	0	0	0	0	0	0	0	0	0	0	0	0	0	0	0	0	0	0	0	0	?
<i>Theope methemona</i>	?	0	0	0	0	0	0	0	0	0	0	0	0	0	0	0	0	0	0	0	0	0	?
<i>Theope sticheli</i>	1	0	0	0	0	0	0	0	0	0	0	0	0	0	0	0	0	0	0	0	0	0	?
<i>Theope bushyi</i>	1	0	0	0	0	0	0	0	0	0	0	0	0	0	0	0	0	0	0	0	0	0	?
<i>Theope turneri</i>	?	0	0	0	0	0	0	0	0	0	0	0	0	0	0	0	0	0	0	0	0	0	?
<i>Theope batesi</i>	1	0	0	0	0	0	0	0	0	0	0	0	0	0	0	0	0	0	0	0	0	0	?
<i>Theope atina</i>	?	0	0	0	0	0	0	0	0	0	0	0	0	0	0	0	0	0	0	0	0	0	?
<i>Theope foliorum</i>	1	0	0	0	0	0	0	0	0	0	0	0	0	0	0	0	0	0	0	0	0	0	?
<i>Theope wallacei</i>	1	0	0	0	0	0	0	0	0	0	0	0	0	0	0	0	0	0	0	0	0	0	?
<i>Theope pakitza</i>	?	0	0	0	0	0	0	0	0	0	0	0	0	0	0	0	0	0	0	0	0	0	?

